Genetically engineered proteins with two active sites for enhanced biocatalysis and synergistic chemo- and biocatalysis

Alonso, Sandra; Santiago, Gerard; Cea-Rama, Isabel; Fernandez-Lopez, Laura; Coscolín, Cristina; Modregger, Jan; Ressmann, Anna K.; Martinez-Martinez, Monica; Marrero, Helena ; Bargiela, Rafael; Pita, Marcos; Gonzalez-Alfonso, Jose L. ; Briand, Manon L. ; Rojo, David; Barbas, Coral; Plou, Francisco J; Golyshin, Peter; Shahgaldian, Patrick; Sanz-Aparicio, Julia ; Guallar, Víctor; Ferrer, Manuel

Nature Catalysis

DOI:
10.1038/s41929-019-0394-4

Published: 01/03/2020

Peer reviewed version

Genetically Engineered Proteins with Two Active Sites for Enhanced Biocatalysis and Synergistic Chemo- and Biocatalysis

Sandra Alonso[1,10], Gerard Santiago[2,10], Isabel Cea-Rama[3,10], Laura Fernandez-Lopez[1], Cristina Coscolín[1], Jan Modregger[4], Anna K. Ressmann[4], Mónica Martínez-Martínez[1], Helena Marrero[1], Rafael Bargiela[5,6], Marcos Pita[1], Jose L. Gonzalez-Alfonso[1], Manon L. Briand[7], David Rojo[8], Coral Barbas[8], Francisco J. Plou[1], Peter N. Golyshin[5,6], Patrick Shahgaldian[7], Julia Sanz-Aparicio[3,11,*], Víctor Guallar[2,9,11,*] and Manuel Ferrer[1,11,*]

[1]Institute of Catalysis, Consejo Superior de Investigaciones Científicas (CSIC), 28049 Madrid, Spain. [2]Barcelona Supercomputing Center (BSC), 08034 Barcelona, Spain. [3]Department of Crystallography & Structural Biology, Institute of Physical Chemistry "Rocasolano", CSIC, 28006 Madrid, Spain. [4]EUCODIS Bioscience GmbH, 1030 Vienna, Austria. [5]School of Natural Sciences, Bangor University, LL57 2UW Bangor, UK. [6]Centre for Environmental Biotechnology, Bangor University, LL57 2UW Bangor, UK. [7]University of Applied Sciences and Arts Northwestern Switzerland, School of Life Sciences, Institute of Chemistry and Bioanalytics, CH-4132 Muttenz, Switzerland. [8]Centro de Metabolómica y Bioanálisis (CEMBIO), Facultad de Farmacia, Universidad CEU San Pablo, 28668 Boadilla del Monte, Madrid, Spain. [9]Institució Catalana de Recerca i Estudis Avançats (ICREA), 08010 Barcelona, Spain. [10]These authors contributed equally: Sandra Alonso, Gerard Santiago, and Isabel Cea-Rama. [11]These authors equally coordinated the work: Julia Sanz-Aparicio, Víctor Guallar and Manuel Ferrer. *e-mail: xjulia@iqfr.csic.es (J.S-A.); victor.guallar@bsc.es (V.G.); mferrer@icp.csic.es (M.F.).

Enzyme engineering has allowed not only de novo creation of active sites catalysing known biological reactions with rates close to diffusion limits, but also the generation of abiological sites performing new-to-nature reactions. However, catalytic advantages of engineering multiple active sites into a single protein scaffold are yet to be established. Here, we report on proteins with two active sites of biological and/or abiological origin, for improved natural and non-natural catalysis. The approach increased catalytic properties, such as enzyme efficiency, substrate scope, stereo-selectivity, and optimal temperature window of an esterase when containing two biological sites. Then, one of the active sites was metamorphosed into a metal-complex chemocatalytic site for oxidation and Friedel-Crafts alkylation reactions facilitating synergistic chemo- and biocatalysis in a single protein. The transformation of 1-naphthyl acetate to 1,4-naphthoquinone (conversion *ca*. 100%) and vinyl crotonate/benzene to 3-phenylbutyric acid (≥83%; e.e. >99.9%) was achieved in one-pot by this artificial multi-functional metalloenzyme.

The field of enzyme engineering has developed considerably over the last decade, opening great potential for applications ranging from greener production processes and diagnostics to therapeutic usage and biomedicine. Directed evolution and computation-driven rational mutagenesis are fostering such developments[1-4]. These techniques allow optimization of biocatalysts by tuning substrate specificity and improving the activity and/or stability under operational conditions. In addition, significant efforts in *de novo* enzymatic active site design are being undertaken, although directed evolution and protein engineering are required to boost the activity of the original computational design. The introduction of biocatalytic sites into non-catalytic protein scaffolds also opens new opportunities[5-9]. As such, certain artificial enzymes approach the diffusion limit while still catalysing the desired reaction using a single artificial active site, with turnover rates as high as those of some natural enzymes (1-5 s^{-1})[10-12].

There are also examples in which catalytically competent organometallic complexes have been introduced in proteins that serve as scaffolds to generate artificial metalloenzymes (ArMs). The first examples of ArMs date back to the late 1970s, when Wilson and Whitesides introduced a diphosphine rhodium (I) biotin derivative into a streptavidin scaffold. The authors demonstrated that this achiral chemocatalyst, located in the asymmetric environment of the biotin-binding site of streptavidin, was capable of chiral hydrogenation of α-acetamido-acrylic acid[13]. However, this work, possibly owing to the unenthusiastic conclusions drawn by the authors, did not attract the attention of the scientific community. It was only the early 2000s that a resurgence of interest in ArMs began, fuelled by advances in both organometallic catalysis and protein engineering[14]. Since then, a large number of ArMs, created through the docking of catalytically competent molecules into protein scaffolds by covalent, supramolecular, dative, and metal substitution, have been described. While the catalytic performance of such ArMs, shown to be competent for catalytic reactions including hydrolysis,

reduction, oxidation, C-C bond-forming and C-heteroatom bond-forming, has long been inferior to that of their natural counterparts, recent efforts combining catalyst design and modern protein engineering allowed bridging of this gap[14,15]. For example, the Ward group developed a directed mutation strategy to produce thousands of protein variants and selected the most active one capable of catalysing metathesis reactions in cells[16]. Additionally, the Roelfes group developed artificial copper-bipyridine catalysts capable of enantioselective Friedel-Crafts alkylation by *in vivo* incorporation, in a protein scaffold, of metal-binding unnatural amino acids[17] or by the creation of an artificial active site capable of copper-binding[18].

Despite significant efforts directed at introducing single artificial biological[5-12] or abiological[13-18] catalytic entities into a protein scaffold, the introduction of multiple active sites, either biological or non-natural, and the analysis of the catalytic advantages it can have, is rare. The only examples are protein scaffolds with two heme, Fe-S or copper sites catalysing the same chemistry[14,18-22], or a recent engineered lipase into which a catalytic metal has been introduced[23]. Although, this last design can potentially confer the capacity for cascade reactions, the catalysis was done in a two-step fashion, changing the reaction conditions, precluding synergistic effects.

Here, we report an approach that exploits the possibility to genetically engineer proteins with two biological actives sites, and furthermore, its expansion allowing its further metamorphosis into a protein with both biological and abiological active sites (Fig. 1). Results are presented demonstrating the broad potential and versatility of the presented procedure to create biocatalysts with improved catalytic properties, and metallo-enzymes capable of cascade reactions where an active synergy of both biological and abiological catalytic entities exists.

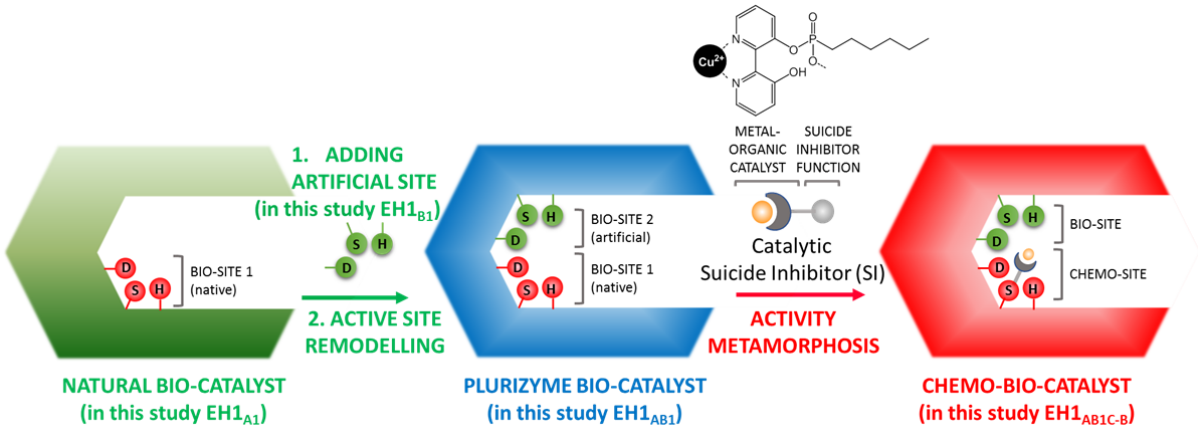

Fig. 1 General concept for engineering proteins with two active sites. The concept consists of the following sequential workflow. First, a target natural enzyme (*e.g.* a serine ester hydrolase in this study), containing a biological active site (BIO-SITE 1 in figure), is selected. Second, by applying Protein Energy Landscape Exploration (PELE) software, an extra potential binding pocket to introduce an artificial biological active site (*e.g.* a nucleophilic serine in this study) is identified, which

can be further remodelled to achieve an optimal configuration (BIO-SITE 2). Third, through the differential affinity for a suicide phosphonate inhibitor bearing a metal-organic complex, one of the biological sites is metamorphosed into a copper-based chemocatalytic (or abiological) site (CHEMO-SITE), while the other site retains its own biological activity.

Results

Design of a protein with two biological active sites and its catalytic advantages

Improving the efficiency of enzymes is rapidly becoming a necessity. One could imagine attacking the problem by engineering more and more reactive sites into a single enzyme scaffold, which by a synergetic effect may improve catalysis. We named this concept as *plurizyme* (the Latin root pluri: multiplicity). However, the first trial of introducing a second artificial active site into a serine esterase containing a natural one could not bring in catalytic advantages (Supplementary Note 1)[24]. Here, through providing a better spatial configuration we designed a new artificial design ($EH1_{B1}$; Supplementary Figure 1) with boosted catalytic performance, in such a way that its incorporation to the natural enzyme ($EH1_{A1}$) intensified the k_{cat} (average: *ca*. 3.4-fold; *max*.: *ca*. 74-fold) and k_{cat}/K_m (average: *ca*. 94-fold; *max*.: *ca*. 5000-fold) for ester hydrolysis, increased the stereo-selectivity by *ca*. 1100-fold (e.e. >99.9%), and broadened by *ca*. 20ºC the temperature at which the enzyme retained more than 80% of the optimal (Fig. 2). It also expanded the substrate spectra, as the resulting *plurizyme* with the two sites ($EH1_{AB1}$) has the ability to hydrolyze all substrates (78, in total) that each site, combined, convert (Supplementary Figure 2).

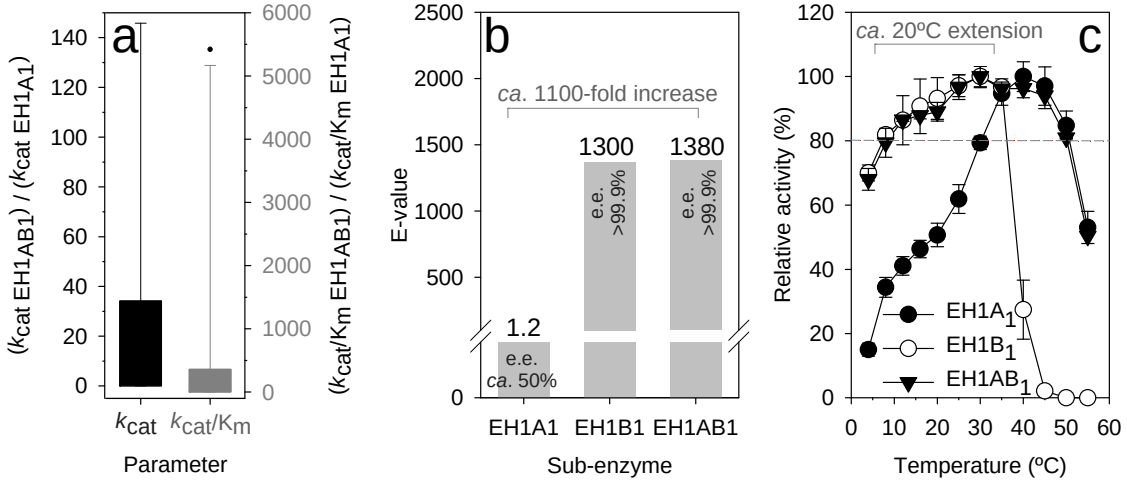

Fig. 2 Bio-catalytic advantages of having two biological active sites. a, The artificial site ($EH1_{B1}$) intensifies the catalytic efficiency. Shown is the blox plot illustrating the relative increase of k_{cat} (left axis) and k_{cat}/K_m (right axis) values of the $EH1_{AB1}$ *plurizyme* with the two sites vs the original $EH1_{A1}$ enzyme with a single active site, for all substrates converted. **b**, The artificial site introduces stereo-specificity. Shown are the average E-values and e.e., determined by gas chromatography, for

the kinetic resolution of a racemic mixture of methyl (2*R*/*S*)-2-phenylpropanoate (*R*-specificity) by the three sub-enzymes. Experimental conditions, raw data and standard deviations for these and other substrates are given in Supplementary Note 2 (Supplementary Figures 2-3, Supplementary Tables 1-2). **c**, The artificial site expands the optimal temperature window. Shown are the temperature profiles of the three sub-enzymes. For T_{opt} determination, calculated on a continuous pH indicator assay[24], conditions are as follows - [protein]: 4.5 µg/ml; [glyceryl tripropionate]: 50 mM; reaction volume: 44 µl; T: 4-55ºC; pH: 8.0. The data, calculated from three independent assays ± standard deviations (calculated using Excel version 2019) and not fitted to any model, represent the relative percentages (%) of specific activity expressed as U mg^{-1}, compared with the maximum.

Together, engineering multiple active sites with identical chemistry catalyzed can thus help, through differences in specificity, affinity, turnover rates and local stabilities, intensifying the original bio-catalytic properties of, or conferring new properties (*e.g.* stereo-specificity and expanded working temperature) to, a natural enzyme, herein exemplified by a serine ester-hydrolase. For detailed description of the engineering approach, and detailed experimental and results information see Supplementary Note 2 (Supplementary Figures 2-3, Supplementary Tables 1-2).

Structural evidences of a *plurizyme* with two biological active sites

To prove that both active sites of our *plurizyme* ($EH1_{AB1}$) are capable of substrate binding and that conversion can occur in both sites, we performed a structural analysis. We obtained crystals from $EH1_{AB1}$ diffracting at 2.1 Å resolution. These crystals were cocrystallized with the suicide inhibitor methyl 4-nitrophenyl hexylphosphonate (M4-4NHP) to obtain the corresponding derivative complex, with two molecules of the inhibitor bound at the catalytic Ser161 (original nucleophile) and Ser211 (artificial nucleophile) sites (Fig. 3a; see Supplementary Note 3, Supplementary Figures 4-6). The 4-nitrophenyl phosphonate inhibitor is susceptible to nucleophilic attack by the catalytic Ser, leading to covalent modification and complete inactivation of the enzyme (see Supplementary Note 4, Supplementary Figure 7)[25,26].

The solved three-dimensional structures show high flexibility in a region (which resembles but does not equal a typical *lid* of lipases) containing the two N-terminal helical regions, Pro4-Gly19 and Ala30-Gly43, which give access to the active-site pocket. Conformational changes are observed at the secondary Ser211 catalytic site, the artificially remodelled site, upon inhibitor binding, as shown in Fig. 3b, which introduce distortions in the packing arrangement within the soaked crystals, explaining the decreased resolution observed (not shown). Nevertheless, the atomic interaction of the inhibitor bound at the two sites can be depicted and is displayed in Fig. 3c-f.

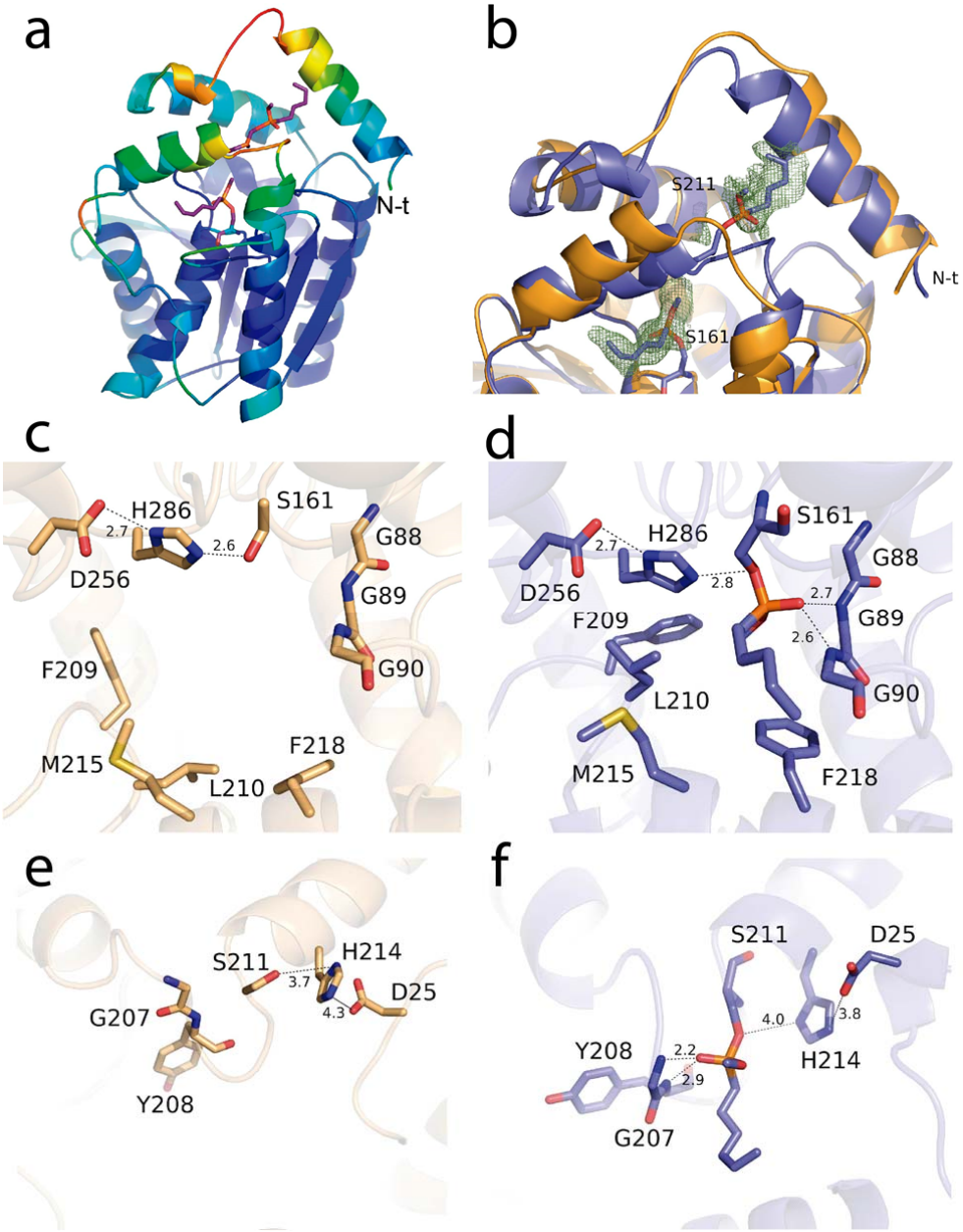

147

148 **Fig. 3 Crystal structure of EH1$_{AB1}$. a**, Cartoon of the crystallized complex coloured by B factors,
149 from low (blue) to high (red) with the two bound molecules from the suicide inhibitor M4-4NHP
150 represented as magenta sticks. **b**, Details of the comparison between the free (orange) and complexed
151 (slate) EH1$_{AB1}$ showing the conformational changes observed in the environment of Ser211 upon
152 inhibitor binding. Polder omit maps calculated at the Ser161 and Ser211 catalytic sites displayed at 3.0
153 σ cut-off. **c-f**, Detail of the Ser161 and Ser 211 binding sites in the free (c, e) and complexed (d, f)
154 crystals showing relevant distances as dashed lines.

155 **Metamorphosis of a *plurizyme* into a protein with biological and abiological active sites**

We further designed an approach to build a protein with both biological and abiological sites supporting different chemistries. For this purpose, here, we used our $EH1_{AB1}$ *plurizyme* as a platform and a suicide inhibition strategy. This approach, also called mechanism-based inhibition, occurs when an enzyme covalently binds a substrate analogue through a reaction similar to that normally catalysed by the enzyme. This reaction is specific and typically occurs with amino acids involved in a catalytic reaction, resulting in enzyme activity loss[25]. In the particular case of ester-hydrolases, esters of phosphonate are long known to stoichiometrically bind to the serine residue of a catalytic triad[26]. Here, a Suicide Inhibitor (SI), 3'-hydroxy-[2,2'-bipyridin]-3-yl methyl hexylphosphonate, equipped with a transition metal-chelating moiety (*e.g.* a bipyridine ligand) was synthesized and used (see Supplementary Note 5, Supplementary Scheme 1, Supplementary Figures 8-10). This approach is expected to confer the inhibitor unit with transition metal-based catalytic function[17,18,27,28], which will be brought into one of the two active sites of a *plurizyme*, while the other remains intact (see Fig. 1).

As in the case of M4-4NHP used for cocrystallization, we found that SI binds to the native (Ser161) and artificial (Ser211) nucleophiles, as the treatment of $EH1_{A1}$, $EH1_{B1}$ and $EH1_{AB1}$ sub-enzymes with an excess of SI resulted in inactivation of >99% in less than 10 min (see Supplementary Note 6, Supplementary Figure 11). To verify the bio-conjugation, the SI-modified sub-enzymes were incubated for 24 h with an excess of $Cu(NO_3)_2$, and the resulting Cu^{2+}-modified sub-enzymes were extensively dialyzed to remove the uncoupled inhibitor and copper (see Supplementary Methods). Further, they were analysed by recording λ_{max} at 386 nm, the redox properties of the Cu^{2+}-organic complex, and the molecular mass by electrospray ionization mass spectrometry (ESI-MS).

We first observed the presence of a λ_{max} at 386 nm in all three modified sub-enzymes (Fig. 4a), which is characteristic of a Cu^{2+}-bipyridine complex (Fig. 4b)[17,18]; this signal was not detected for the proteins without copper addition (Fig. 4a).

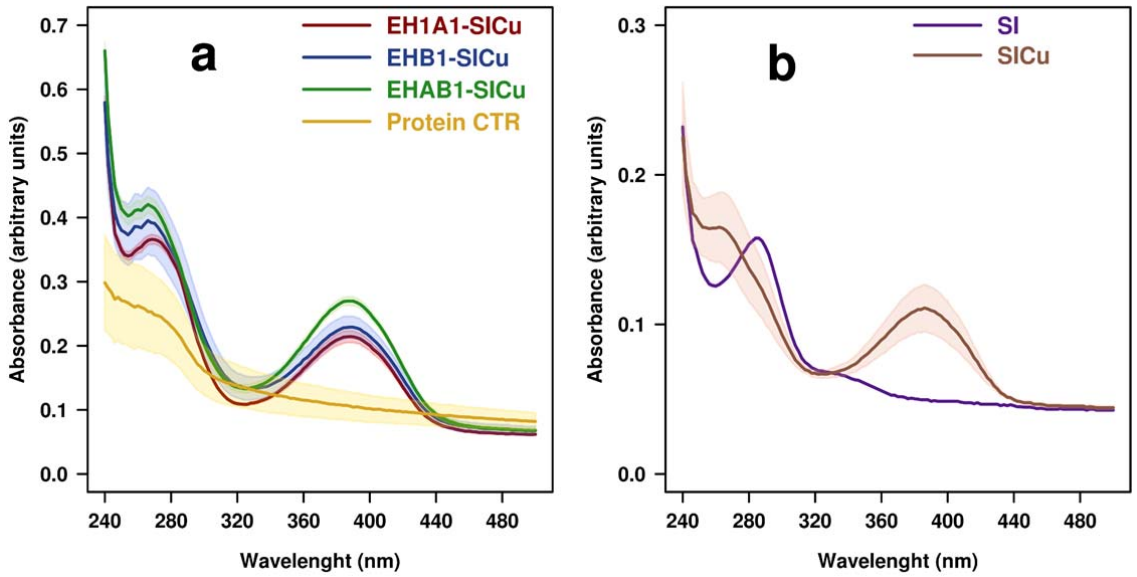

Fig. 4 Absorption spectra of modified and un-modified sub-enzymes. a, Incorporation of Cu^{2+}-SI (SICu) as detected by UV-vis spectroscopy. Spectra were recorded in 96-well plates using Cu^{2+}-modified sub-enzymes (15 μM) prepared with an excess (120 μM) of inhibitor and Cu^{2+} (see Supplementary Methods) in a total volume of 200 μl. Modified sub-enzymes prepared with an excess (120 μM) of inhibitor but without copper salt are shown as a control. **b**, The UV-vis spectra of SI and Cu-modified SI inhibitor (SICu) at 15 μM in a total volume of 200 μl. Shown are average values with a standard deviation of triplicates (calculated using Excel version 2019) shown as shadows; in the case of the control sample, the average value and standard deviation of all three sub-enzymes measured in triplicate are shown.

By recording the cyclic voltammetry electrochemical response on 3-mercaptopropanoic acid (MPA)-modified gold electrodes (Supplementary Note 6, Supplementary Figure 12), we further observed a different behaviour between the free Cu^{2+}-organic complex and the SICu complex, which shows an expected lower electrochemical reversibility due to the chelation of the Cu^{2+} cation in the SI chelating pocket (Supplementary Note 6, Supplementary Figure 13). When SICu was located in the protein scaffold (Fig. 6a) the copper electrochemical signal became more reversible. Results not only showed that the copper complex is effectively inside the corresponding sub-enzymes active sites, but that the electrochemical peaks have shifted and the copper redox signals differs when located in each sub-enzyme (Fig. 6a). Such differences are better spotted in the sub-enzyme with two active sites ($EH1_{AB1}$) which, due to the presence of two binding Cu^{2+} sites, has an extra increase in the signal of Cu^{2+} compared to sub-enzymes A1 ($EH1_{A1}$) and B1 ($EH1_{B1}$) which contains only one. It is also worth pointing out that there is no electrochemical response at the free SICu potentials, suggesting that the inhibitor does not leak out of the binding pocket. The recording of the oxidation of catechol also showed a higher catechol oxidation activity of the $EH1_{AB1}$-SICu biocatalyst compared $EH1_{A1}$-CuSI and $EH1_{B1}$-CuSI (Fig. 6b), not observed in the absence of CuSI (Fig. 6b inset). Catechol did not behave as electrochemical substrate and the process does not fulfil all the requirements to be considered a bioelectrocatalytic oxidation process; however, the enzymes behave as an electron transfer relay that allows the oxidation of catechol at its non-catalytic potential (0.25V *vs* Ag/AgCl; see Supplementary Note 6). Impedance spectroscopy measurements were also performed using catechol as the redox electrochemical probe. Impedance spectroscopy showed a similar trend for each sub-enzyme: modified sub-enzymes displayed in every case a lower electron transfer resistance than non-modified ones. Nyquist plots allow calculating the charge transfer resistance (Rct) between the electrodes modified with each sub-enzyme and the catechol (Fig. 6c). Remarkably, the $EH1_{AB1}$–SICu sub-enzyme offered a 10-fold reduction in the Rct when compared to that of $EH1_{AB1}$ in the absence of SICu, a 3-fold reduction in the Rct when compared to that of $EH1_{A1}$–SICu and a 4-fold reduction in the Rct when compared to that of $EH1_{B1}$–SICu. These results suggest that the two active sites of the $EH1_{AB1}$ sub-enzymes contain Cu^{2+}-organic complexes which, because their proximity, facilitates

intramolecular electron transfer at levels higher than those shown by modified $EH1_{A1}$ and $EH1_{B1}$ sub-enzymes containing only one site and one complex (Fig. 6c). Control experiments recorded with the electrodes modified with enzymes lacking CuSI, which yielded no electrochemical response of catechol, support the need of CuSI-socketed enzymes to allow an electronic path to the electrode surface. Such electronic path is more likely intramolecular, as there is no sign of CuSI leakage, and an extramolecular electron path would imply the cooperation of different enzymes, a less likely mechanism. For detailed description of the electrochemical characterization and electrode and probe design see Supplementary Note 6 (Supplementary Figures 12-18).

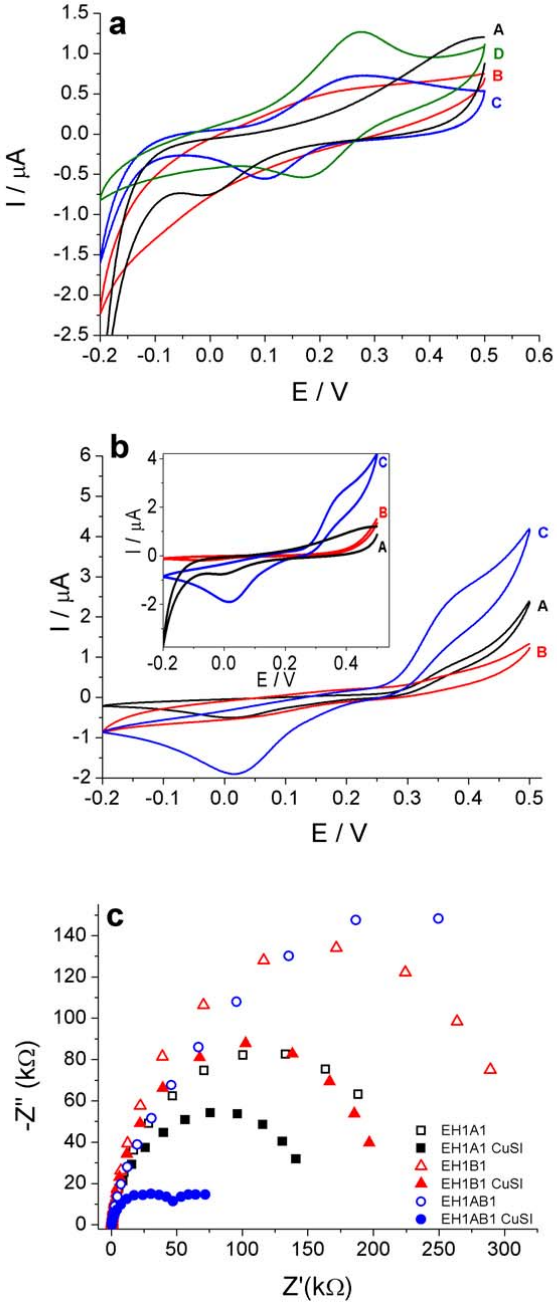

Fig. 5 Electrochemical characterization of the chemo-bio catalysts. a, Electrochemical signals of MPA-gold electrodes modified with (A) CuSI, (B) $EH1_{A1}$-CuSI, (C) $EH1_{B1}$-CuSI and (D) $EH1_{AB1}$-CuSI. The CuSI concentration added was *ca*. 0.43 mM. All measurements were recorded using a 20 $mV \cdot s^{-1}$ scan rate and 50 mM phosphate buffer pH 6.5 electrolyte. The working electrode was a gold disk with a 0.2 cm^2 diameter modified with an MPA SAM. The reference electrode was 3 M Ag/AgCl, and the counter electrode was Pt wire. **b,** Oxidation of catechol (1 mM) by MPA-gold electrodes modified with (A) $EH1_{A1}$-CuSI, (B) $EH1_{B1}$-CuSI and (C) $EH1_{AB1}$-CuSI (process from 0.3 to 0.5 V). Inset: electrochemical responses to catechol measured with MPA-gold electrodes modified with (A) CuSI, (B) $EH1_{AB1}$ in absence of CuSI and (C) $EH1_{AB1}$ in presence of CuSI. **c,** Impedance spectroscopy showing that $EH1_{AB1}$-CuSI presents a much lower electron transfer resistance than any other combination of sub-enzymes with or without CuSI. Impedance measurements were performed using catechol 1 mM, a bias potential of 0.35 V *vs* Ag/AgCl. The experimental setup (sub-enzyme concentration *ca*. 0.43 mM) was the same 3-electrode configuration used for cyclic voltammetry.

Together, results confirm that the SI herein synthesized can be used as a platform to introduce a Cu^{2+}-organic complex into our genetically engineered *plurizyme* through the elimination of the methoxy group of the suicide inhibitor and the coupling of a 3'-hydroxy-[2,2'-bipyridin]-3-yl moiety capable of copper binding. The bio-conjugation of two organic complexes to $EH1_{AB1}$ and one to $EH1_{A1}$ and $EH1_{B1}$ was also confirmed by ESI-MS (Supplementary Note 6, Supplementary Figure 19).

The fact that, under excess conditions, the conjugation occurs at both active sites might be a disadvantage, as our primary objective was to create a *plurizyme* variant, hereafter referred to as $EH1_{AB1}$ chemo-biocatalyst ($EH1_{AB1C\text{-}B}$), in which one of the active sites is replaced by a Cu^{2+}-catalyst and the other remains unaltered. To remedy this shortcoming, we evaluated the possibility that both sites have different affinities for the inhibitor; the different affinities for multiple other substrates (see Supplementary Note 2, Supplementary Figure 2) and the differences in catalytic environments of each active site (Fig. 3) indicated such a possible differentiation. This hypothesis was evaluated by measuring the loss of hydrolytic activity of each sub-enzyme ($EH1_{A1}$, $EH1_{B1}$ and $EH1_{AB1}$) in the presence of different concentrations of the inhibitor. As shown in Supplementary Note 7 (see Supplementary Figure 20), whereas the native site could be inhibited at very low concentrations (*ca*. 5 µM), the artificial one was only inhibited at concentrations above 35 µM. On the basis of the differential active-site affinity, a dose-dependent inhibition strategy was designed that allowed the specific bio-conjugation of the Cu^{2+}-organic complex to Ser161 but not to Ser 211 (see Supplementary Methods; Supplementary Note 7, Supplementary Figure 21). As such, an $EH1_{AB1}$ variant in which the Cu^{2+}-organic complex was bio-conjugated at the native active site but not the artificial site could be obtained (Fig. 6), with a coupling efficiency and purity higher than 98% (see Supplementary Note 7,

Supplementary Figures 22-23). This result was confirmed by applying this strategy to each of the sub-enzymes and by confirming the increase in mass by ESI-MS and the λ_{max} at 386 nm by UV/vis absorption spectroscopy (see Supplementary Note 7, Supplementary Figures 22-24). As an additional experimental confirmation, we cocrystallized $EH1_{AB1}$ with the CuSI complex (see Supplementary Note 3, Supplementary Figure 6). Despite its moderate resolution (2.79 Å), the electron density confirmed binding of the ligand only to the native active site. However, the poor quality at the copper-bipyridine moiety impeded modelling of this portion, which might be attributed to disorder or partial occupancy.

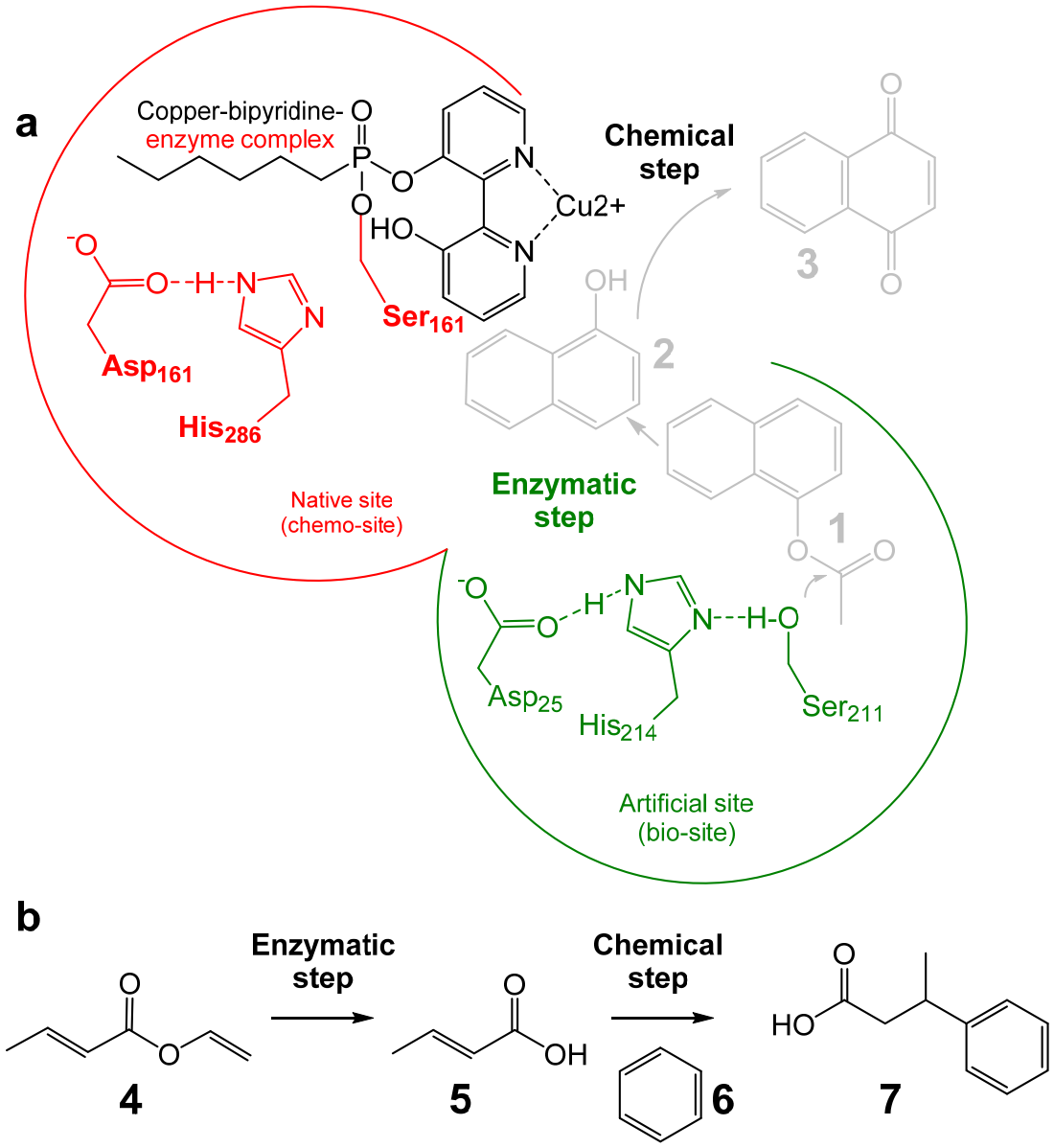

Fig. 6 Image representing the chemo-biocatalyst $EH1_{AB1C-B}$ generated in this study and its utilization in two model reactions. a, Schematic representation of the $EH1_{AB1C-B}$ design. Colour code

as follows: green, the artificial enzymatic site; red: the native site; black: copper-bipyridine molecule placed in the native site. In grey colour, the one-pot conversion of 1-naphthyl acetate (**1**) to naphthol (**2**) by the enzymatic site and its further oxidation to 1,4-naphthoquinone (**3**) by the metal-complex site are illustrated. **b,** Model one-pot conversion of vinyl crotonate (**4**) to crotonic acid (**5**) by the enzymatic site, and its further Friedel-Crafts alkylation to β-phenylbutyric acid (**7**) by the metal-complex site in the presence of benzene (**6**).

Synergistic catalysis of the biological with the abiological active site

The catalytic activity of $EH1_{AB1C\text{-}B}$ (Fig. 6a) was evaluated in 2 cascade reactions, which consist of the enzymatic hydrolysis of an ester, followed by a copper-bipyridine oxidation (Fig. 6a, in grey colour) or a Friedel-Crafts alkylation reaction (Fig. 6b). In the first target reaction, enzymatic hydrolysis of ester **1** will produce alcohol **2**, which may be oxidized by the copper-bipyridine catalyst to quinone **3**. This reaction was selected based on the fact that electrochemical tests demonstrated an electron transfer capacity by copper-bipyridine. Ester **1** was selected because it is a polyphenol ester for which the artificial esterase site shows a high conversion rate (see Supplementary Note 2, Supplementary Figure 2, Supplementary Table 1). In the second target reaction, enzymatic hydrolysis of ester **4** will produce the alkenyl fatty acid **5**, which in the presence of benzene (**6**) may yield β-phenylbutyric acid (**7**)[40]. This model reaction was selected because copper-bipyridine catalysts have been shown to perform vinylogous Friedel-Crafts alkylation reactions[17,18]; ester **4** was selected because it was well converted by the artificial site (see Supplementary Note 2, Supplementary Figure 2, Supplementary Table 1), and the resulting hydrolysis product can be coupled with benzene.

The first reaction (Fig. 6a) was carried out at pH 8.0 and 25ºC using 10 mM ester **1**. Using a modified protein not containing Cu^{2+}, no quinone **3** was formed, but formation of alcohol **2** (100% conversion) was found (Fig. 7a). This result was expected because the only active site was the biocatalytic site. However, in the presence of the chemo-biocatalyst, the conversion to quinone **3** reached 100% after a 2 h reaction (Fig. 7b). The second reaction (Fig. 6b) was carried out at 4ºC for 3 days following conditions described elsewhere[17,18]. Using a modified protein not containing Cu^{2+}, only crotonic acid (**5**) was formed, and benzene (**6**) remained without consumption (Fig. 8a), whereas in the presence of the chemo-biocatalyst, the conversion reached 83% for product **7** after 3 days (Fig. 8b). The high activity level of the artificial ester-hydrolase active site (Fig. 2c; see Supplementary Note 2, Supplementary Figure 3) at 4ºC helps achieve a high conversion rate for the enzymatic step and the concomitant production of product **7**. Interestingly, the product was obtained with a 99% e.e. for (*S*)-3-phenylbutyric acid (see Supplementary Methods). Reaction mixtures obtained in all cases were analysed by ESI–MS (see Supplementary Methods), and the existence of the reaction products was confirmed in each case. We would like to mention that the reaction conditions were not optimized.

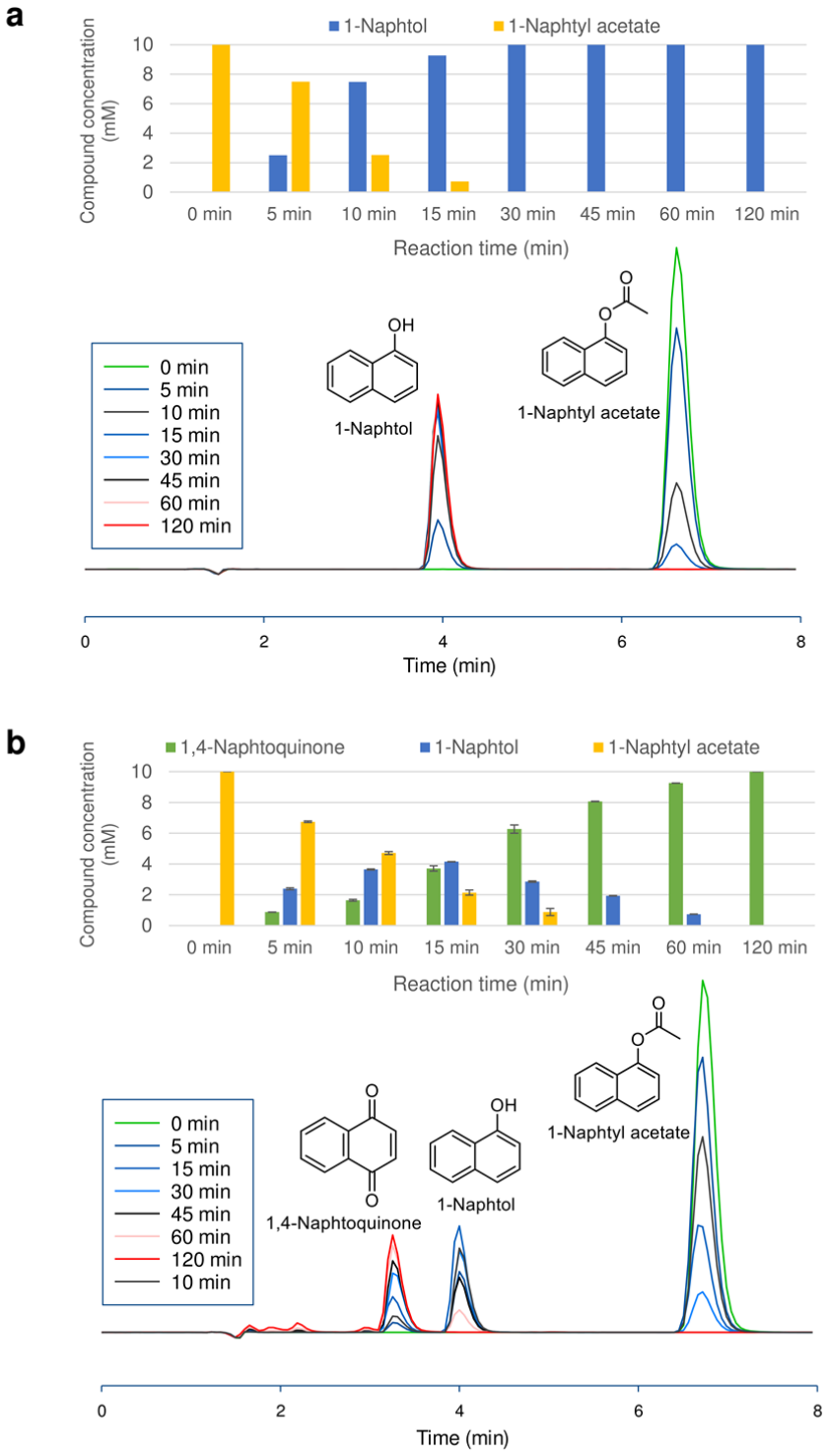

Fig. 7 One-pot synthesis of 1,4-naphthoquinone from 1-napthyl acetate catalysed by $EH1_{AB1C-B}$. a, Control reaction performed with modified sub-enzyme not containing Cu^{2+}. **b**, Reaction in the presence of $EH1_{AB1C-B}$ containing Cu^{2+}. Reaction conditions as follows: - [1-naphthyl acetate]: 10 mM; [sub-enzyme]: 80 µM; T: 25ºC; pH: 7.0. Reactions were performed in triplicates with average value and standard deviations (calculated using Excel version 2019) indicated.

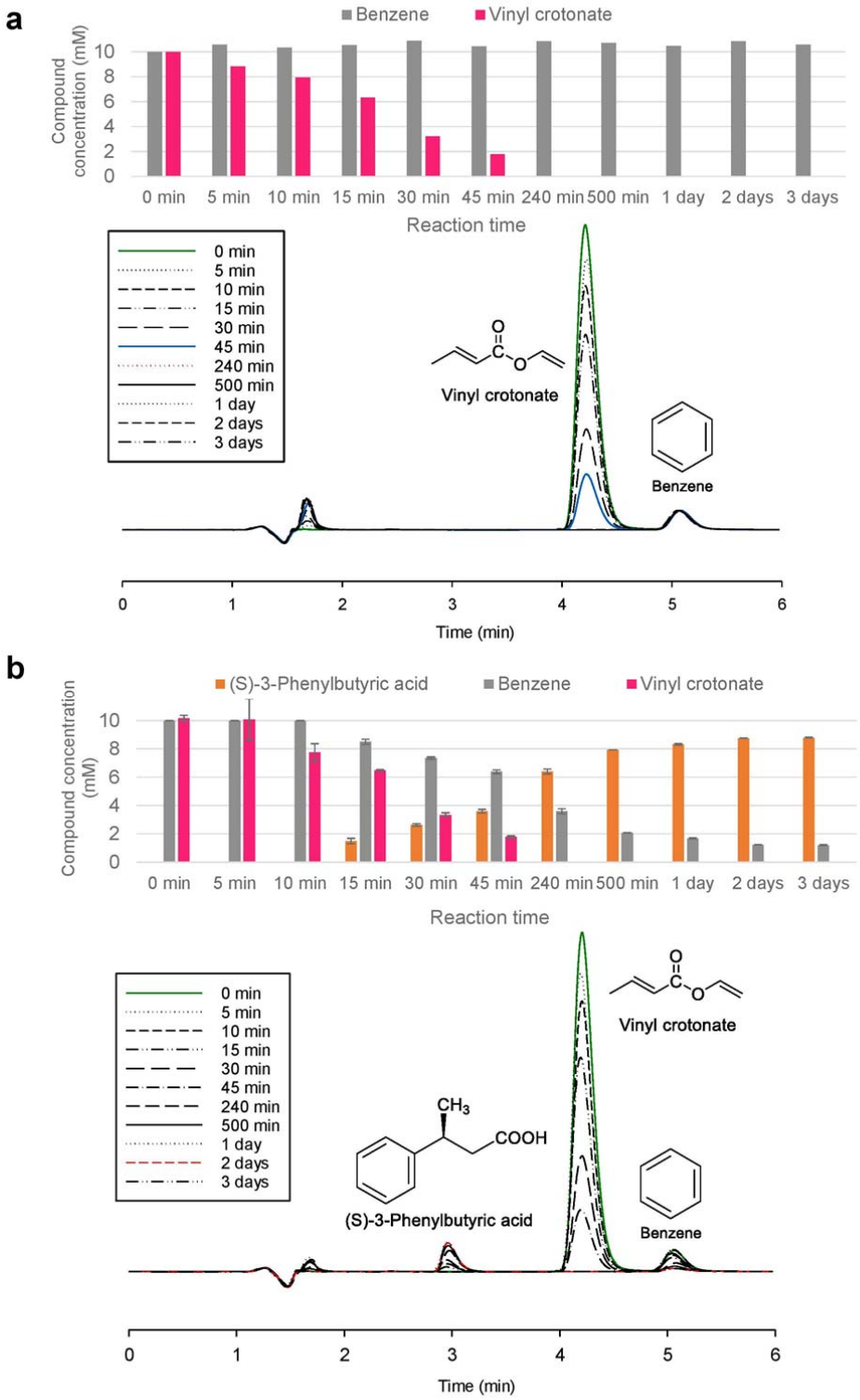

Fig. 8 One-pot synthesis of 3-phenylbutyric acid from vinyl crotonate and benzene catalysed by $EH1_{AB1C-B}$. a, Control reaction performed with modified sub-enzyme not containing Cu^{2+}. **b**, Reaction in the presence of $EH1_{AB1C-B}$ containing Cu^{2+}. Reaction conditions as follows: - [vinyl

crotonate]: 10 mM; [benzene]: 10 mM; [sub-enzyme]: 80 μM; T: 4ºC; pH: 7.0**.** Crotonic acid (intermediate reaction product) is not detected under our analytical method and is not shown. Reactions were performed in triplicates with average value and standard deviations (calculated using Excel version 2019) indicated.

The above two examples demonstrated that a protein scaffold with both biological and abiological sites is capable of performing hydrolytic-oxidative and hydrolytic-alkylation one-pot reactions with excellent conversion and enantio-selectivity. From a catalytic point of view, the approach for creating such hybrid catalysts opens novel opportunities compared to previous designs of bio-inspired chemo-catalysts, in which the protein scaffold is mostly a container of a transition metal-complex whose properties are influenced by the microenvironment where it is positioned within the protein scaffold[18]. Here, the enzyme also contributes to the catalytic activity. Also, compared to the recent design of a lipase with a Cu^{2+} catalyst[23], where the synergy is not direct and requires, after a first hydrolytic step mediated by the lipase activity, a second reduction reaction just requiring Cu^{2+} and $NaBH_4$ added to a concentration (*ca*. 15 mg/ml) which may compromise protein integrity and catalyst reutilization[41]; thus, in the second reaction the protein does not play an active catalytic role except to immobilize the Cu^{2+} catalyst. In contrast, in our design the reaction is done in one step allowing synergetic catalysis and easy handling; also the cascade reaction produce products in high e.e. that cannot be achieved by the metal cofactor without the protein scaffold.

From a methodological point of view, the strategy designed herein to introduce transition metal-complexes can complement the ones previously described, including the metal-binding utilizing cysteine conjugation[18,23] or unnatural amino acids[17]. It is worth mentioning the following advantages. First, our strategy, requiring only side chain replacement, is expected to be versatile in that it can potentially be applied to a large range of enzymes. Second, through the application of PELE simulations, we ensure that the metal-catalyst is located in an area capable of substrate binding[42]. Third, the metal-catalyst is incorporated through a well stablished suicide inhibition mechanism only requiring the presence of a nucleophilic serine. While introducing two nucleophilic serine may create selectivity problems that do not exist for other bio-conjugation approaches[18,23], it is also true that both may have different affinities by which one can control the coupling specificity, as it was shown in the *plurizyme* herein designed. It is also plausible that both sites may have different specificity for other metal-complexes allowing specific bio-conjugation, yet to be investigated, or that in other *plurizymes* to be developed such selectivity problems may not occur because different active site configurations. For additional remarks see Supplementary Note 7.

Conclusions

Recent progress in (bio)chemical sciences has enabled the design and production of protein scaffolds artificially endowed with either biocatalytic or chemocatalytic activities. While this is plausible when

a single artificial catalytic entity is introduced into a protein scaffold, it is however challenging to introduce multiple sites and activities, including natural and non-natural ones. To what extend can additional sites and activities, either biological and/or abiological, intensify the catalytic performance of protein scaffolds? Overcoming this challenge and finding answers to this question would allow the design of more efficient biocatalysts with improved natural activities and multi-catalytic systems for performing non-natural concerted cascade reactions.

Here, an approach to design catalytically active proteins equipped with two enzymatic active sites or an enzymatic and a chemocatalytic site is described, and consists of the following sequential workflow: production of a genetically engineered *plurizyme* with two distinct active sites (e.g. two sites supporting ester hydrolysis in this study) through structure-based modelling – chemical design of a synthetic catalytic suicide inhibitor capable of coordinating a transition metal ion – metamorphosis of one of the serine hydrolytic biological sites into a versatile metal-complex chemocatalytic site through suicide inhibition. We hypothesized this approach may provide technical advantages, including expansion of the diversity of artificial catalysts, and new catalytic opportunities. This was showed by a first example demonstrating that the catalytic properties of a natural serine hydrolase can be significantly boosted by adding an artificial site with an appropriate catalytic configuration, because the additive effect of the two biological (natural and artificial) sites. Results provided in Supplementary Note 8 (Supplementary Figures 25-28, Supplementary Table 3) further demonstrated that the *plurizyme* approach and the catalytic enhancement associated to the introduction of multiple biological sites is reproducible and can be easily extended to other serine ester-hydrolase. A second example is also exemplified by the design of hybrid homogeneous catalysts integrating multi-catalytic units in one, which are capable of performing chemical and biological catalysis in synergy (*e.g.*, sequential reactions) with excellent conversion and enantio-selectivity. Results provided in Supplementary Note 9 (Supplementary Figures 29-31, Supplementary Table 4) further demonstrated that our design offers advantages compared to traditional multi-catalyst systems[23], as the co-localization of both biological and abiological catalytic entities in a single scaffold was shown to favour substrate and product transfer of one to another and to expand the performance under conditions at which the native catalysts are sub-optimal.

Methods

A full description of the methods is available in the Supplementary Information (see Supplementary Methods, and Supplementary Note 10, Supplementary Figures 32-36).

Data availability: The atomic coordinates have been deposited in the Protein Data Bank under accession numbers 6I8F, 6RB0 and 6RKY. All other data is available from the authors upon reasonable request.

References

1. Bren, K. L. Engineered biomolecular catalysts. *J. Am. Chem. Soc*. **139**, 14331-14334 (2017).
2. Ebert, M. C. & Pelletier, J. N. Computational tools for enzyme improvement: why everyone can - and should - use them. *Curr. Opin. Chem. Biol.* **37**, 89-96 (2017).
3. Arnold, F. H. Directed evolution: Bringing new chemistry to life. *Angew Chem. Int. Ed. Engl.* **57**, 4143-4148 (2018).
4. Acebes, S. et al. Rational enzyme engineering through biophysical and biochemical modeling. *ACS Catal*. **6**, 1624-1629 (2016).
5. Seelig, B. & Szostak, J. W. Selection and evolution of enzymes from a partially randomized non-catalytic scaffold. *Nature* **448**, 828-831 (2007).
6. Jiang, L. et al. De novo computational design of retro-aldol enzymes. *Science* **319**, 1387-1391 (2008).
7. Richter, F. et al. Computational design of catalytic dyads and oxyanion holes for ester hydrolysis. *J. Am. Chem. Soc.* **134**, 16197-16206 (2012).
8. Rufo, C. M. et al. Short peptides self-assemble to produce catalytic amyloids. *Nat. Chem*. **6**, 303-309 (2014).
9. Moroz, Y. S. et al. New tricks for old proteins: single mutations in a nonenzymatic protein give rise to various enzymatic activities. *J. Am. Chem. Soc*. **137**, 14905-14911 (2015).
10. Blomberg, R. et al. Precision is essential for efficient catalysis in an evolved Kemp eliminase. *Nature* **503**, 418-421 (2013).
11. Khersonsky, O. et al. Optimization of the in-silico-designed Kemp eliminase KE70 by computational design and directed evolution. *J. Mol. Biol.* **407**, 391-412 (2011).
12. Röthlisberger, D. et al. Kemp elimination catalysts by computational enzyme design. *Nature* **453**, 190-195 (2008).
13. Wilson, M. E. & Whitesides, G. M. Conversion of a protein to a homogeneous asymmetric hydrogenation catalyst by site-specific modification with a diphosphinerhodium(I) moiety. *J. Am. Chem. Soc.* **100**, 306-307 (1978).
14. Dydio, P. et al. An artificial metalloenzyme with the kinetics of native enzymes. *Science,* **354**, 102-106 (2016).
15. Lewis, J. C. Artificial metalloenzymes and metallopeptide catalysts for organic synthesis. *ACS Catal*. **3**, 2954-2975 (2013).
16. Jeschek, M. et al. Directed evolution of artificial metalloenzymes for in vivo metathesis. *Nature* **537**, 661-665 (2013).
17. Drienovská, I. et al. Novel artificial metalloenzymes by *in vivo* incorporation of metal-binding unnatural amino acids. *Chem Sci*. **6**, 770-776 (2015).
18. Bos, J. et al. Enantioselective artificial metalloenzymes by creation of a novel active site at the protein dimer interface. *Angew. Chem. Int. Ed. Engl.* **51**, 7472-7475 (2012).

19. Lin, Y.-W. et al. Rational design of heterodimeric protein using domain swapping for myoglobin. *Angew. Chem. Int. Ed.* **54**, 511– 515 (2015).
20. Farid, T. A. Elementary tetrahelical protein design for diverse oxidoreductase functions. *Nat. Chem. Biol.* **9**, 826-833 (2013).
21. Roy, A. et al. De novo design of an artificial bis[4Fe-4S] binding protein. *Biochemistry* 2013, 52, 7586-7594 (2013).
22. Tebo, A. G. & Pecoraro, V. L. Artificial metalloenzymes derived from three-helix bundles. *Curr. Opin. Chem. Biol.* **25**, 65-70 (2015).
23. Felice, M. et al. Synthesis of a heterogeneous artificial metallolipase with chimeric catalytic activity. *Chem. Commun. (Camb)* **51**, 9324-9327 (2015).
24. Santiago, G. et al. Rational engineering of multiple active sites in an ester hydrolase. *Biochemistry* **57**, 2245-2255 (2018).
25. Zollner H. *Handbook of enzyme inhibitors* (Wiley-VCH Verlag GmbH, 1999).
26. Myers, D. K. Competition of the aliesterase in rat serum with the pseudo cholinesterase for diisopropyl fluorophosphonate. *Science* **115**, 568-570 (1952).
27. Beller M., Renken A. & van Santen R. A. *Catalysis: from principles to applications* (Wiley-VCH Verlag GmbH, 2012).
28. Schwizer, F. et al. Artificial metalloenzymes: reaction scope and optimization strategies. *Chem. Rev.* **118**, 142-231 (2018).
29. Wang, T. et al. Rational redesign of the active site of selenosubtilisin with strongly enhanced glutathione peroxidase activity. *J. Catal.* **359**, 27-35 (2018).
30. Hoque, M. A. et al. Stepwise loop insertion strategy for active site remodeling to generate novel enzyme functions. *ACS Chem. Biol*. **12**, 1188-1193 (2017).
31. Payer, S. E. et al. A rational active-site redesign converts a decarboxylase into a C=C hydratase: "Tethered Acetate" supports enantioselective hydration of 4-hydroxystyrenes. *ACS Catal.* **8**, 2438-2442 (2018).
32. Zastrow, M. L. & Pecoraro, V. L. Influence of active site location on catalytic activity in de novo-designed zinc metalloenzymes. *J. Am. Chem. Soc*. **135**, 5895-5903 (2013).
33. Ross, M. R. et al. Histidine orientation modulates the structure and dynamics of a de novo metalloenzyme active site. *J. Am. Chem. Soc*. **137**, 10164-10176 (2015).
34. Der, B. S., Edwards, D. R. & Kuhlman, B. Catalysis by a de novo zinc-mediated protein interface: implications for natural enzyme evolution and rational enzyme engineering. *Biochemistry* **51**, 3933-3940 (2012).
35. Khare, S. D. et al. Computational redesign of a mononuclear zinc metalloenzyme for organophosphate hydrolysis. *Nat. Chem. Biol*. **8**, 294-300 (2012).
36. Zastrow, M. L. et al. Hydrolytic catalysis and structural stabilization in a designed metalloprotein. *Nat. Chem*. **4**, 118-123 (2012).

37. Dydio, P. et al. An artificial metalloenzyme with the kinetics of native enzymes. *Science* **354**, 102-106 (2016).
38. Zandonella, G. et al. Interactions of fluorescent triacylglycerol analogs covalently bound to the active site of a lipase from *Rhizopus oryzae*. *Eur. J. Biochem.* **262**, 63-69 (1999).
39. Tokuriki, N. et al. Diminishing returns and tradeoffs constrain the laboratory optimization of an enzyme. *Nat. Commun.* **3**, 1257 (2012).
40. Koelsch C. F., Hochmann H., Le Claire C. D. The Friedel-Crafts reaction with cinnamic, crotonic, and β-chlorocrotonic acids. *J. Am. Chem. Soc.* **65**, 59-60 (1943).
41. Blanco R. M. & Guisán J. M. Stabilization of enzymes by multipoint covalent attachment to agarose-aldehyde gels. Borohydride reduction of trypsin-agarose derivatives. *Enzyme Microb. Technol*. **11**, 360-366 (1989).
42. Lecina D., Gilabert J. F. & Guallar V. Adaptive simulations, towards interactive protein-ligand modeling. *Sci Rep.* **7**, 8466 (2017).

Acknowledgements

This work was funded by grant 'INMARE' from the European Union's Horizon 2020 (grant agreement no. 634486), grants PCIN-2017-078 (within the Marine Biotechnology ERA-NET), CTQ2016-79138-R, BIO2016-76601-C3-1-R, BIO2016-76601-C3-3-R, BIO2017-85522-R, RTI2018-095166-B-I00, and RTI2018-095090-B-100 from the Ministerio de Economía y Competitividad, Ministerio de Ciencia, Innovación y Universidades (MCIU), Agencia Estatal de Investigación (AEI), Fondo Europeo de Desarrollo Regional (FEDER) and European Union (EU). P.N.G. and R.B. acknowledge the support of the UK Biotechnology and Biological Sciences Research Council (BBSRC; grant No. BB/M029085/1) and the Centre of Environmental Biotechnology Project and the Supercomputing Wales project, which are partly funded by the European Regional Development Fund (ERDF) via the Welsh Government. The authors gratefully acknowledge financial support provided by the ERDF. C. Coscolín thanks the Ministerio de Economía y Competitividad and FEDER for a PhD fellowship (Grant BES-2015-073829). Jose L. Gonzalez-Alfonso thanks the support of Spanish Ministry of Education, Culture and Sport through the National Program FPU (FPU17/00044). I. Cea-Rama thanks the Regional Government of Madrid for a fellowship (PEJ_BIO_AI_1201). Authors would like to acknowledge Sergio Ciordia and María C. Mena for MALDI-TOF/TOF analysis. We thank the staff of the European Synchrotron Radiation Facility (ESRF), Grenoble, France, for providing access and for technical assistance at beamline ID30A-1/MASSIf-1 and the Synchrotron Radiation Source at Alba (Barcelona, Spain) for assistance at BL13-XALOC beamline. Authors would like to acknowledge also to María J. Vicente and Maite A. Pascual at the Servicio Interdepartamental de Investigación (SIDI) from the Autonomous University of Madrid for the ESI-MS analyses.

Author contributions

SA, GS and IC-R contributed equally to this work. The manuscript was written through contributions of M. Ferrer, V. Guallar, J. Sanz-Aparicio and P. Shahgaldian. All authors have given approval to the final version of the manuscript. SA, CC, LF-L, MM-M, HM and PNG contributed to site-directed mutagenesis and protein expression, purification and characterization. JM and AKR coordinated, in collaboration with MF, the synthesis of suicide inhibitor. RB contributed to the biochemical data analysis. DR and CB contributed GC analysis for enantioselectivity determination. JLG-A and FJP performed HPLC analysis of the reaction products. GG and VG conducted the PELE simulations and molecular dynamics. MP contributed together with SA and LF-L to the electrochemical measurement. IC-R and JS-A performed the crystallization and X-ray structure determination. MB contributed to protocol development for the inhibition procedure. MF and VG conceived the *plurizyme* work, and MF and PS conceived the metamorphosis of the enzymatic to chemical catalyst. MF wrote the initial draft of the manuscript, which was further written through contributions of VG, JS-A and PS.

Competing interests

The authors declare no competing interests.

Additional information

Supplementary information in available for this paper.

Materials and correspondence should be sent to M. F., V. G. or J. S-A.

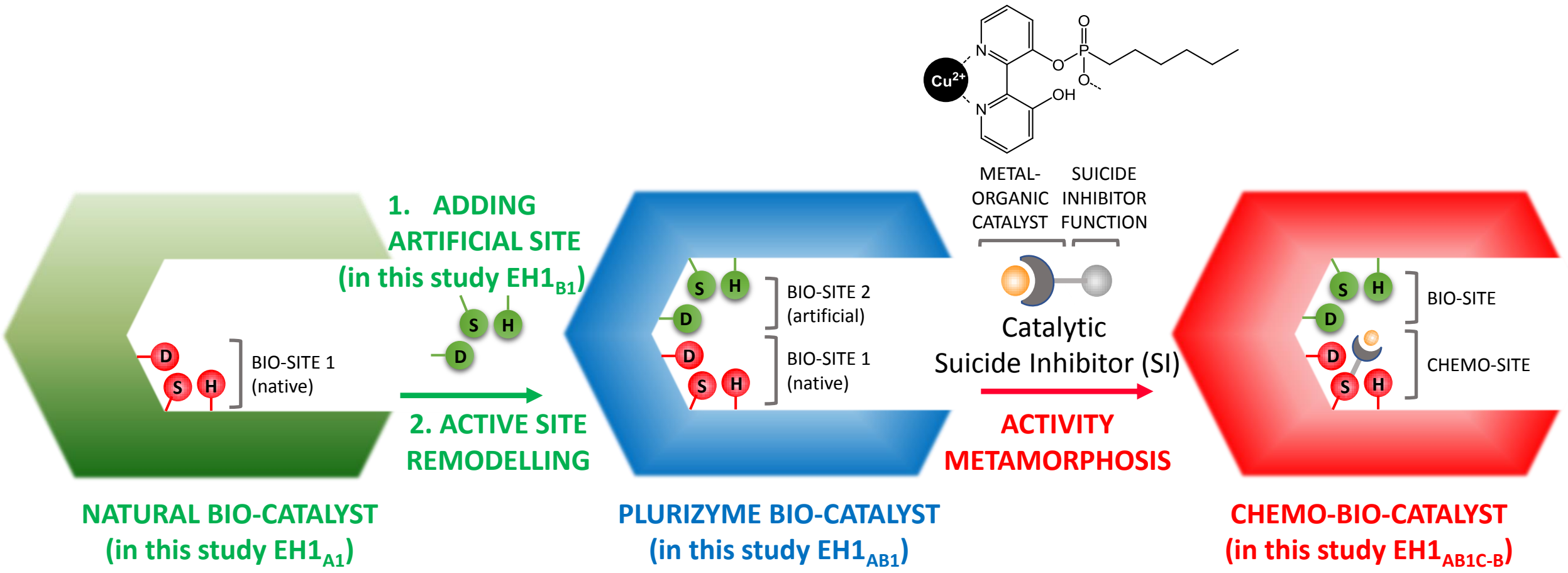
1. ADDING ARTIFICIAL SITE (in this study EH1B1)
2. ACTIVE SITE REMODELLING
BIO-SITE 1 (native)
BIO-SITE 2 (artificial)
BIO-SITE 1 (native)
METAL-ORGANIC CATALYST
SUICIDE INHIBITOR FUNCTION
Catalytic Suicide Inhibitor (SI)
ACTIVITY METAMORPHOSIS
BIO-SITE
CHEMO-SITE
NATURAL BIO-CATALYST (in this study EH1A1)
PLURIZYME BIO-CATALYST (in this study EH1AB1)
CHEMO-BIO-CATALYST (in this study EH1AB1C-B)

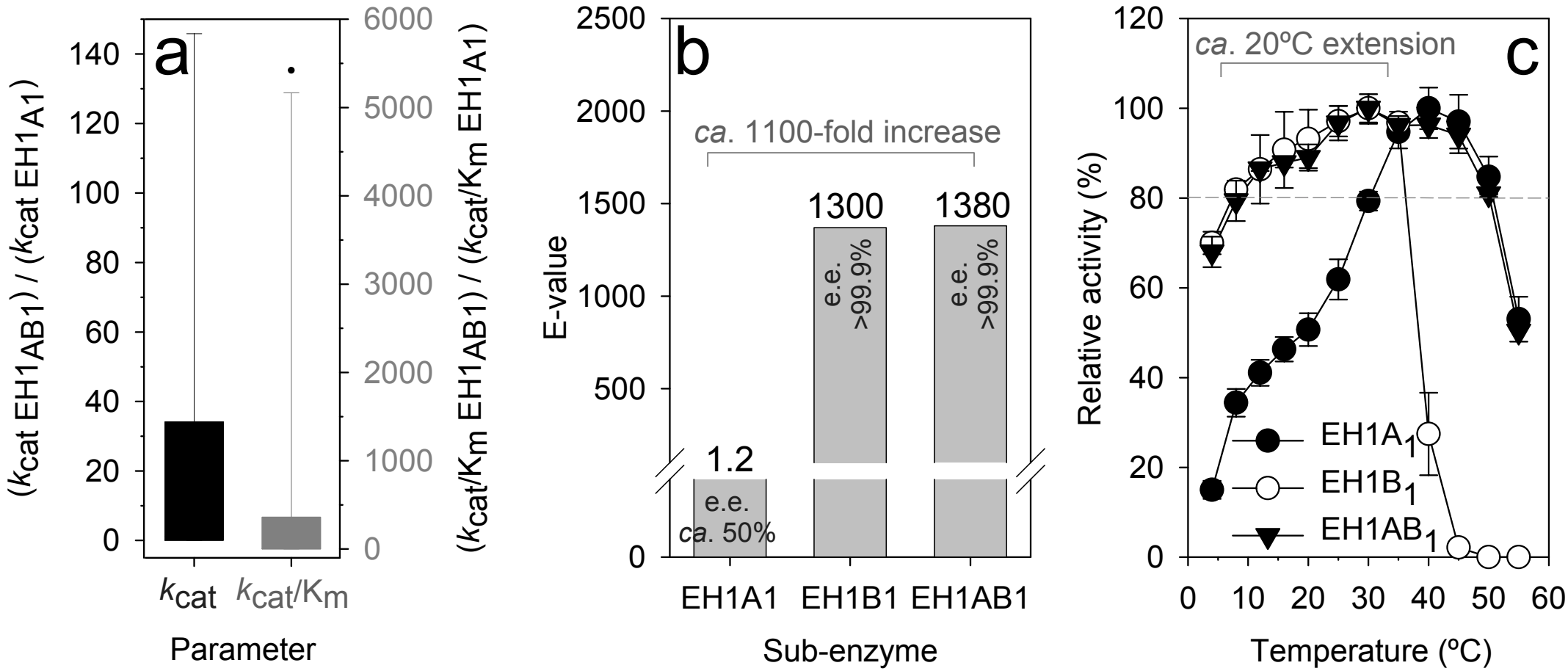
a
(k_{cat} EH1AB1) / (k_{cat} EH1A1)
(k_{cat}/K_m EH1AB1) / (k_{cat}/K_m EH1A1)
k_{cat}
k_{cat}/K_m
Parameter
b
E-value
ca. 1100-fold increase
1.2
e.e. ca. 50%
1300
e.e. >99.9%
1380
e.e. >99.9%
EH1A1
EH1B1
EH1AB1
Sub-enzyme
c
ca. 20ºC extension
Relative activity (%)
EH1A1
EH1B1
EH1AB1
Temperature (ºC)

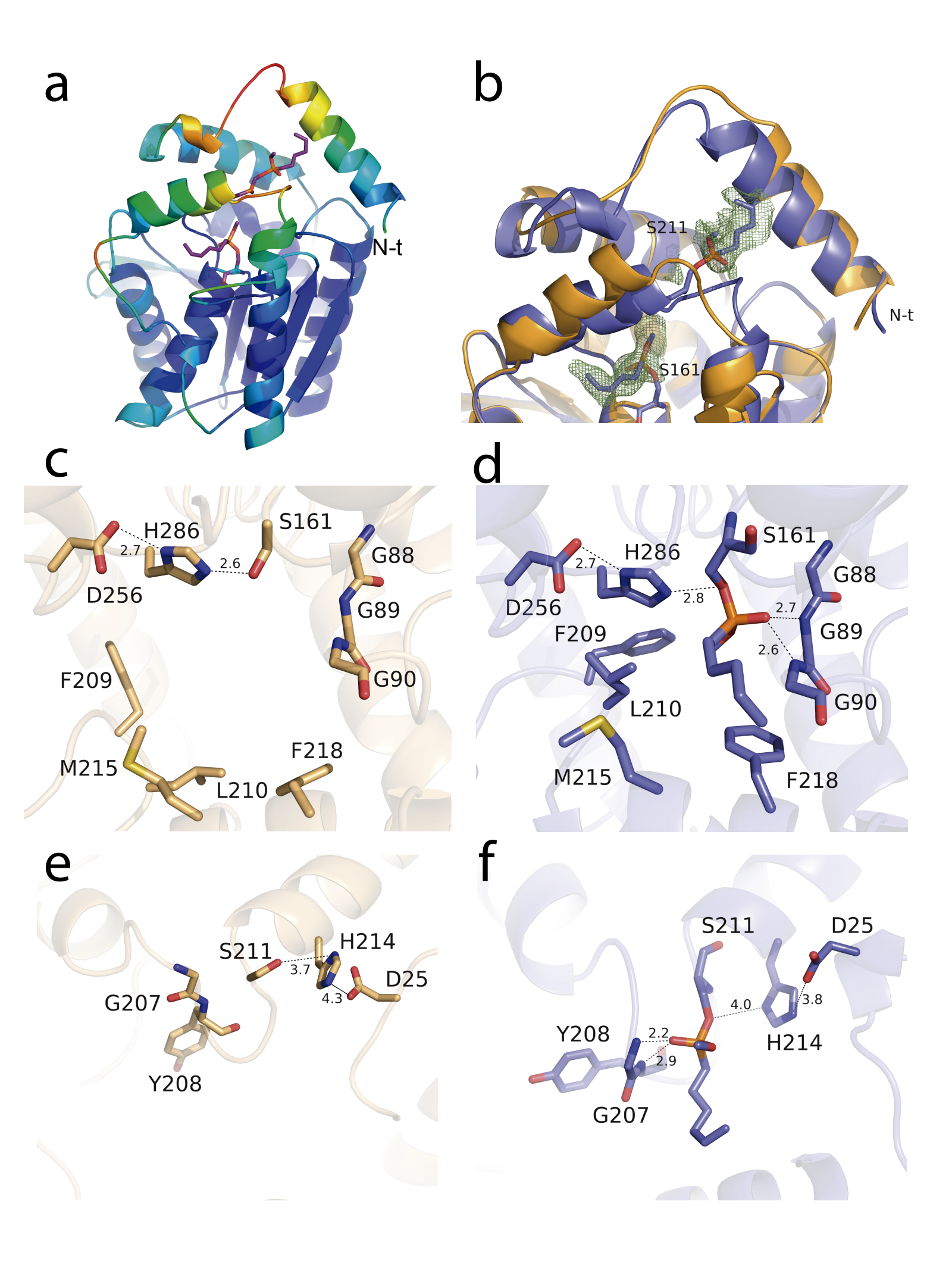
a
N-t
b
S211
S161
N-t
c
H286
2.7
2.6
S161
G88
D256
G89
F209
G90
M215
L210
F218
d
H286
2.7
S161
G88
D256
2.8
2.7
F209
G89
2.6
L210
G90
M215
F218
e
S211
3.7
H214
D25
4.3
G207
Y208
f
S211
D25
4.0
3.8
Y208
2.2
H214
2.9
G207

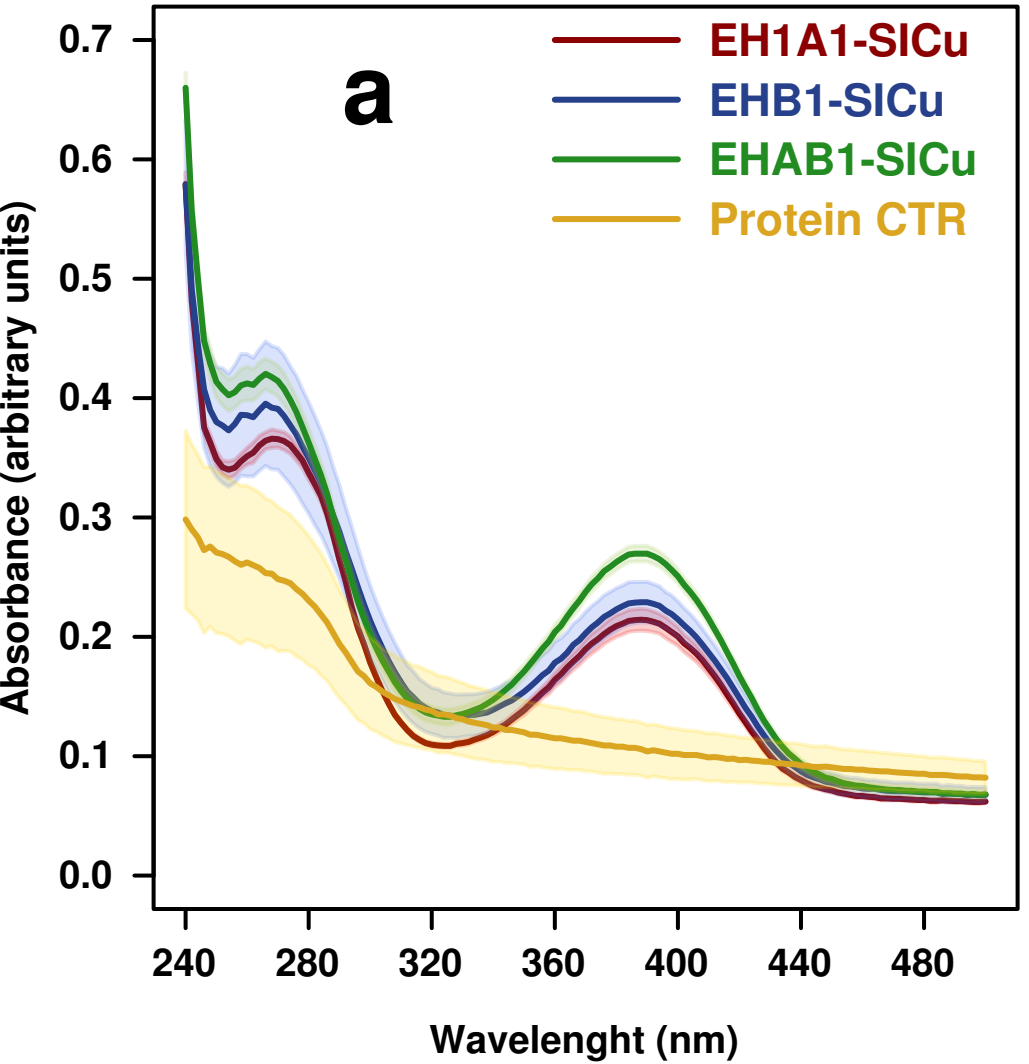
a
EH1A1-SlCu
EHB1-SlCu
EHAB1-SlCu
Protein CTR
Absorbance (arbitrary units)
0.0
0.1
0.2
0.3
0.4
0.5
0.6
0.7
240
280
320
360
400
440
480
Wavelenght (nm)

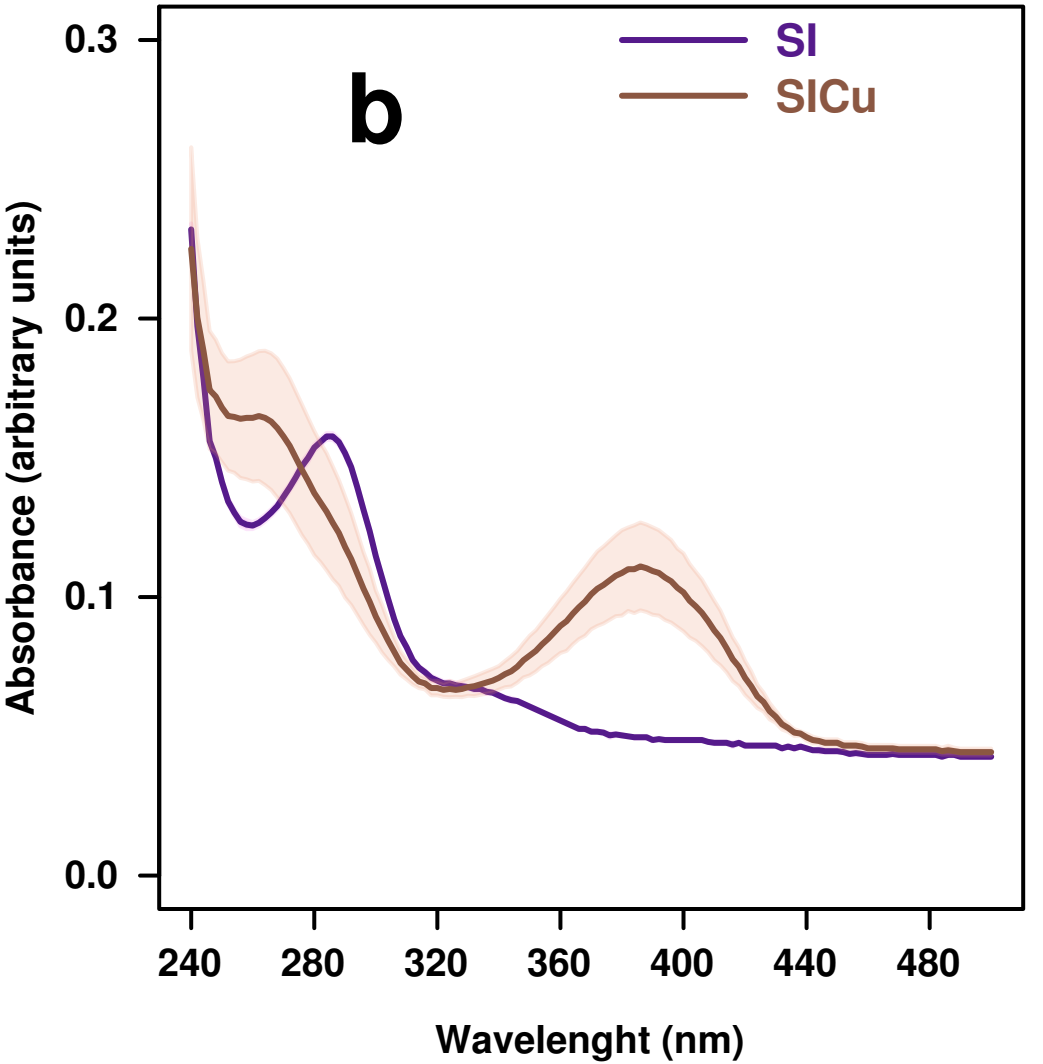
b
Sl
SlCu
Absorbance (arbitrary units)
0.0
0.1
0.2
0.3
240
280
320
360
400
440
480
Wavelenght (nm)

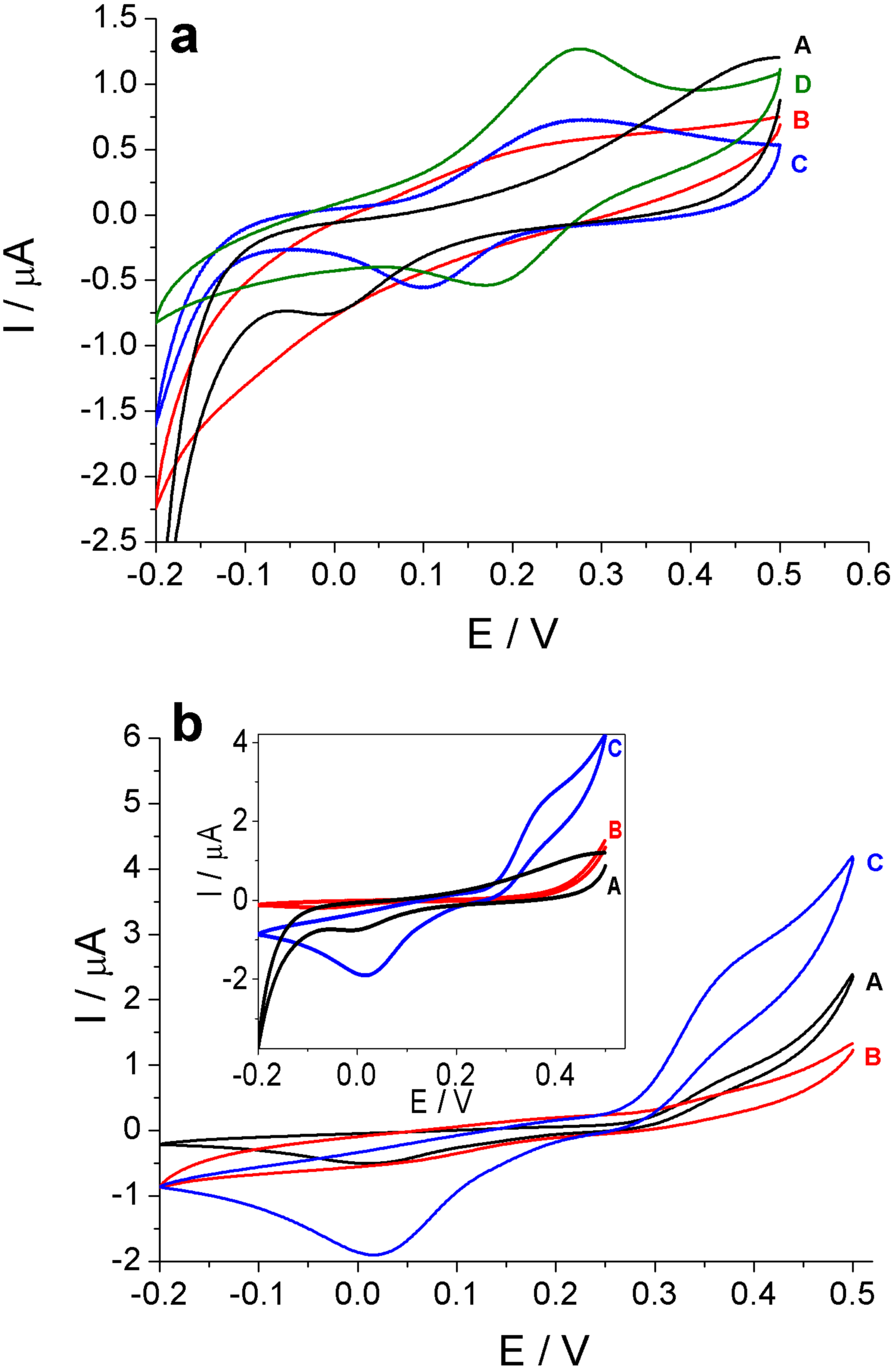
a
A
D
B
C
I / µA
E / V
b
C
B
A
I / µA
E / V
c
EH1A1
EH1A1 CuSI
EH1B1
EH1B1 CuSI
EH1AB1
EH1AB1 CuSI
-Z'' (kΩ)
Z'(kΩ)

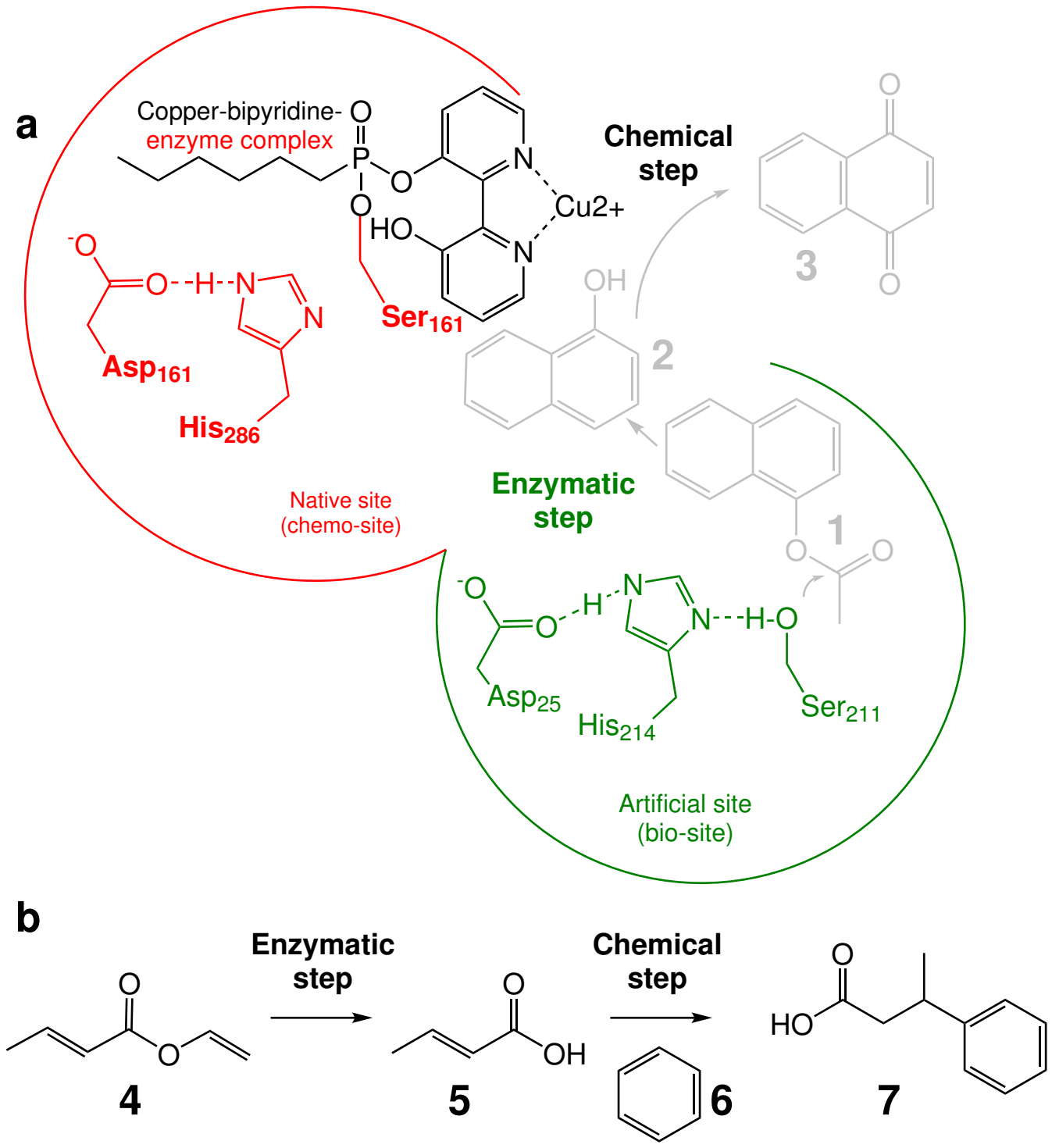
a
Copper-bipyridine-
enzyme complex
Chemical
step
Cu2+
Ser161
Asp161
His286
Native site
(chemo-site)
Enzymatic
step
Asp25
His214
Ser211
Artificial site
(bio-site)
1
2
3
b
Enzymatic
step
Chemical
step
4
5
6
7

a

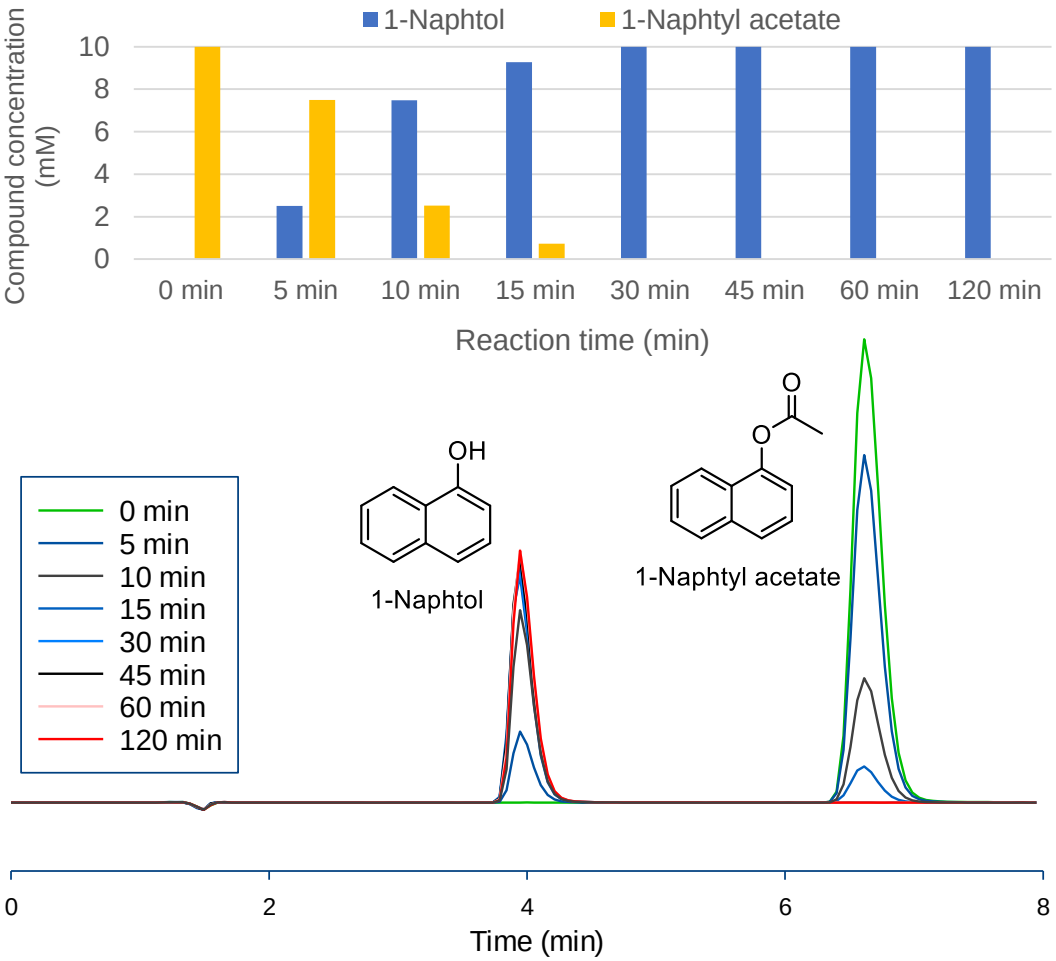
1-Naphtol
1-Naphtyl acetate
Compound concentration (mM)
10
8
6
4
2
0
0 min
5 min
10 min
15 min
30 min
45 min
60 min
120 min
Reaction time (min)
OH
1-Naphtol
O
O
1-Naphtyl acetate
0 min
5 min
10 min
15 min
30 min
45 min
60 min
120 min
0
2
4
6
8
Time (min)

b

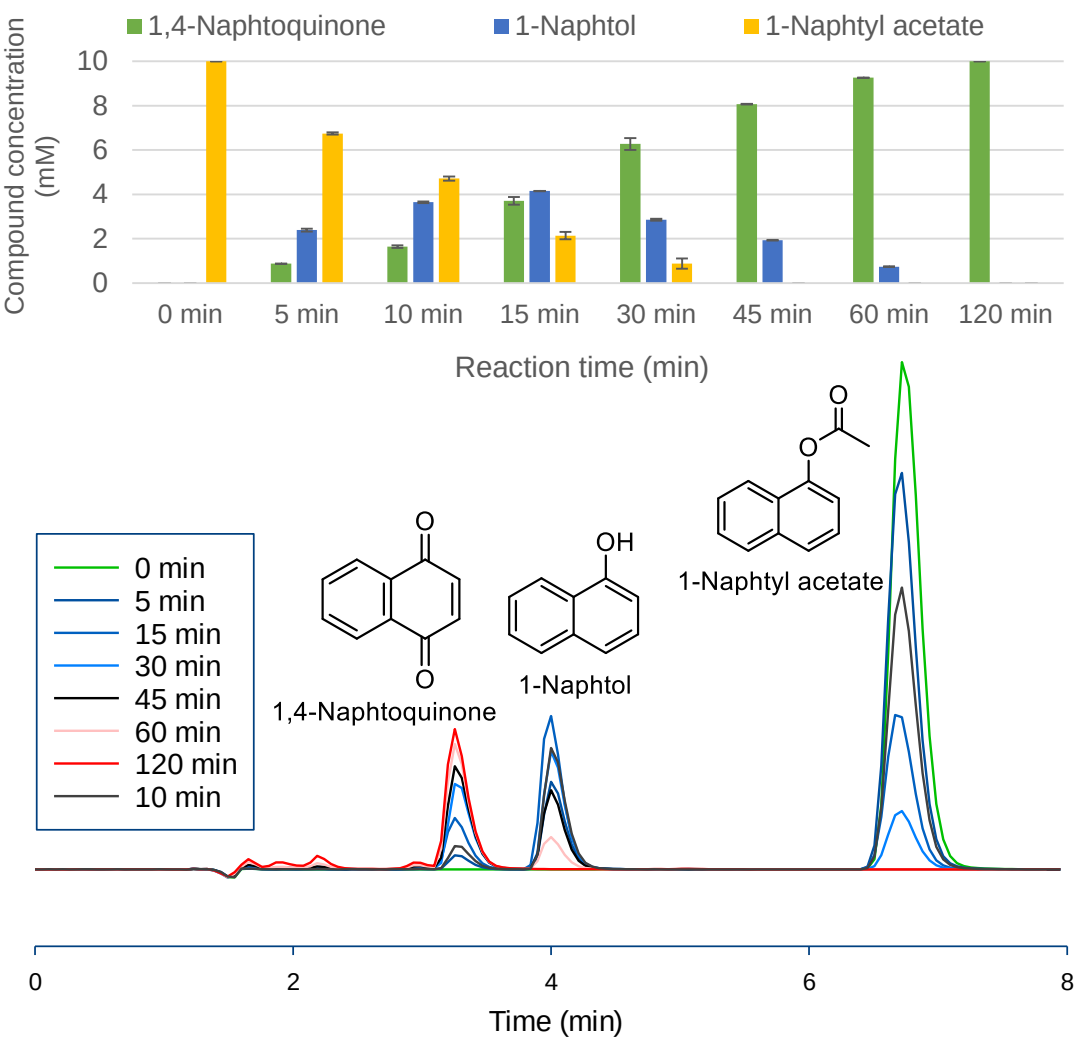
1,4-Naphtoquinone
1-Naphtol
1-Naphtyl acetate
Compound concentration (mM)
10
8
6
4
2
0
0 min
5 min
10 min
15 min
30 min
45 min
60 min
120 min
Reaction time (min)
0 min
5 min
15 min
30 min
45 min
60 min
120 min
10 min
O
O
1,4-Naphtoquinone
OH
1-Naphtol
O
O
1-Naphtyl acetate
0
2
4
6
8
Time (min)

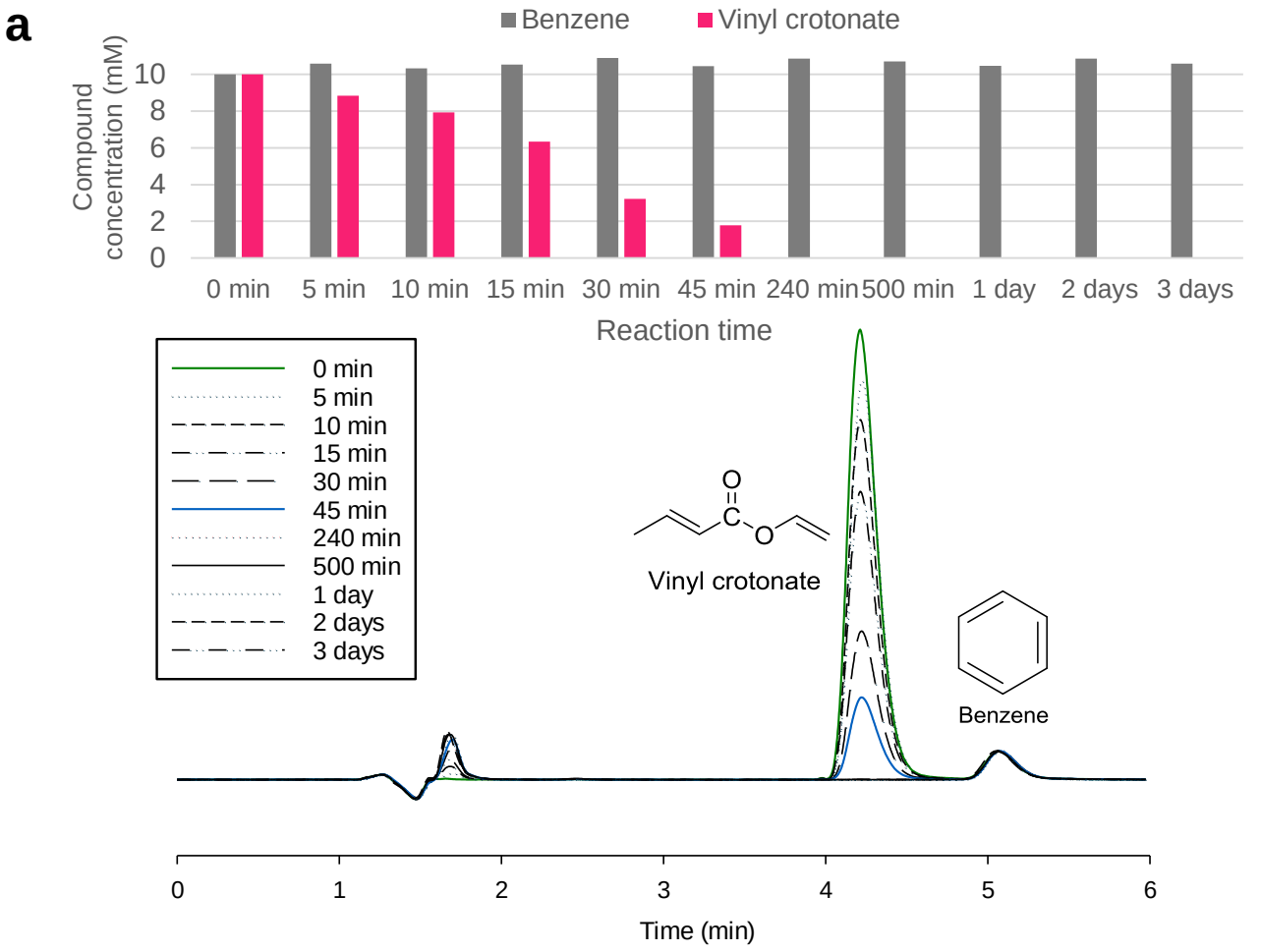
a
Benzene
Vinyl crotonate
Compound concentration (mM)
0 min
5 min
10 min
15 min
30 min
45 min
240 min
500 min
1 day
2 days
3 days
Reaction time
Vinyl crotonate
Benzene
Time (min)

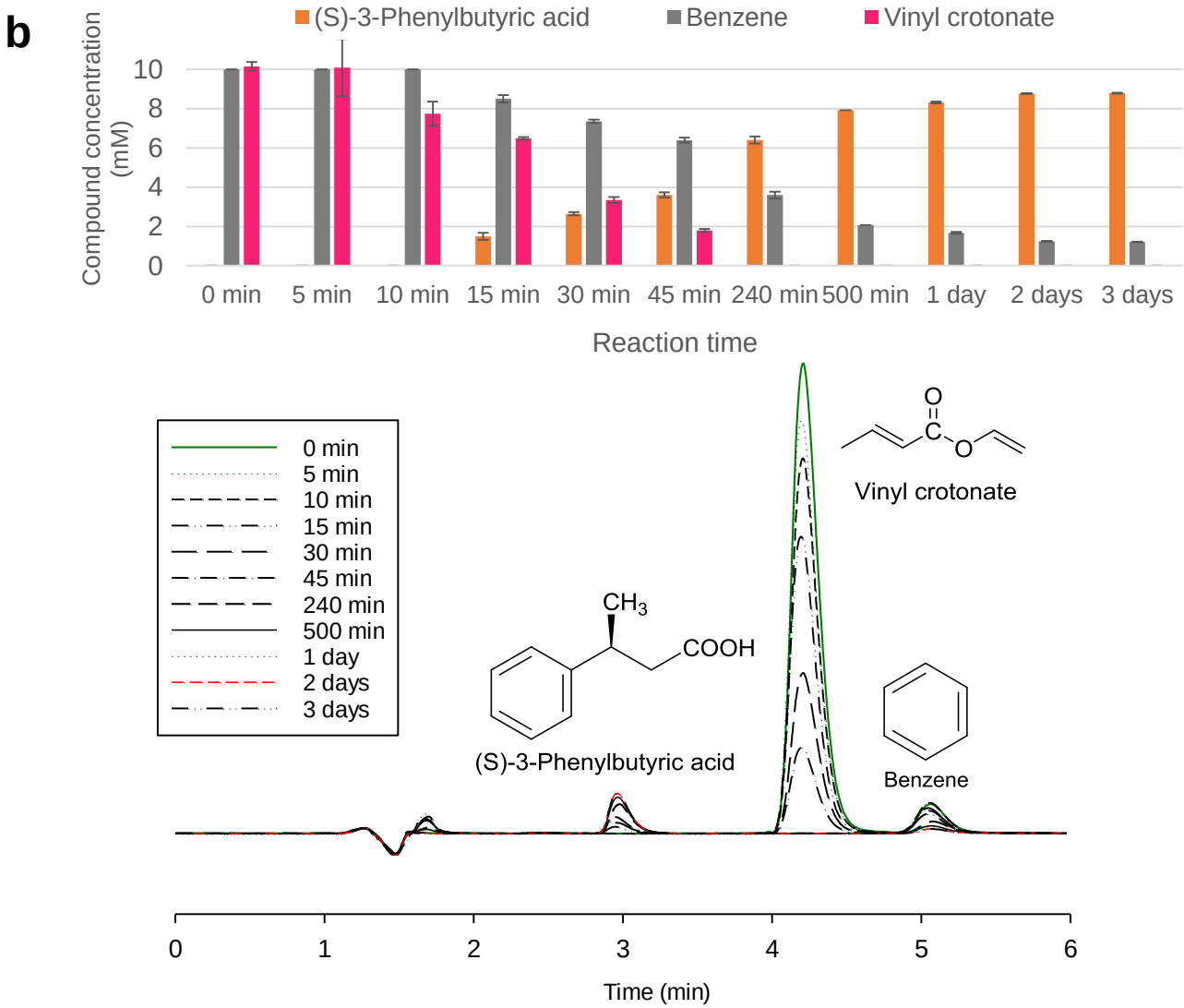
b
(S)-3-Phenylbutyric acid
Benzene
Vinyl crotonate
Compound concentration (mM)
0 min
5 min
10 min
15 min
30 min
45 min
240 min
500 min
1 day
2 days
3 days
Reaction time
Vinyl crotonate
(S)-3-Phenylbutyric acid
Benzene
Time (min)